

FAISAL, N.H., RAJENDRAN, V., PRATHURU, A., HOSSAIN, M., MUTHUKRISHNAN, R., BALOGUN, Y., PANCHOLI, K., HUSSAIN, T., LOKACHARI, S., HORRI, B.A. and BANKHEAD, M. 2024. Thermal spray coatings for molten salt facing structural parts and enabling opportunities for thermochemical cycle electrolysis. *Engineering reports* [online], 6(9), article number e12947. Available from: <https://doi.org/10.1002/eng2.12947>

Thermal spray coatings for molten salt facing structural parts and enabling opportunities for thermochemical cycle electrolysis.

FAISAL, N.H., RAJENDRAN, V., PRATHURU, A., HOSSAIN, M., MUTHUKRISHNAN, R., BALOGUN, Y., PANCHOLI, K., HUSSAIN, T., LOKACHARI, S., HORRI, B.A. and BANKHEAD, M.

2024


© 2024 The Author(s). *Engineering Reports* published by John Wiley & Sons Ltd. This is an open access article under the terms of the Creative Commons Attribution License, which permits use, distribution and reproduction in any medium, provided the original work is properly cited.

 OpenAIR
@RGU

This document was downloaded from
<https://openair.rgu.ac.uk>



Thermal spray coatings for molten salt facing structural parts and enabling opportunities for thermochemical cycle electrolysis

Nadimul Haque Faisal¹  | Vinooth Rajendran¹ | Anil Prathuru¹ |
Mamdud Hossain¹ | Ramkumar Muthukrishnan¹ | Yakubu Balogun¹ |
Ketan Pancholi¹ | Tanvir Hussain² | Siddharth Lokachari² |
Bahman Amini Horri³ | Mark Bankhead⁴

¹School of Engineering, Robert Gordon University, Aberdeen, UK

²Faculty of Engineering, University of Nottingham, Nottingham, UK

³Department of Chemical & Process Engineering, University of Surrey, Guildford, UK

⁴National Nuclear Laboratory, Chadwick House, Warrington, UK

Correspondence

Nadimul Haque Faisal, School of Engineering, Robert Gordon University, Garthdee Road, Aberdeen AB10 7GJ, UK.
Email: n.h.faisal@rgu.ac.uk

Funding information

ScotGov's Emerging Energy Transition Fund (EETF), Grant/Award Number: EETF/HIS/APP/007 (Hy-One); Henry Royce Institute via Materials Challenge Accelerator Programme, Grant/Award Number: MCAPO34 (METALYSIS); Thermochemical electrolysis related funding by UK National Nuclear Laboratory (NNL) via gamechanger, Grant/Award Number: GC 596 (THERMOSIS); Leverhulme Trust Research Fellowship, Grant/Award Number: LTRF2021\17131; UKRI EPSRC, Grant/Award Number: EP/W033178/1 (METASIS)

Abstract

Thermochemical water splitting stands out as the most efficient techniques to produce hydrogen through electrolysis at a high temperature, relying on a series of chemical reactions within a loop. However, achieving a durable thermochemical cycle system poses a significant challenge, particularly in manufacturing suitable coating materials for reaction vessels and pipes capable of enduring highly corrosive conditions created by high-temperature molten salts. The review summarizes thermally sprayed coatings (deposited on structural materials) that can withstand thermochemical cycle corrosive environments, geared towards nuclear thermochemical copper–chlorine (Cu–Cl) cycles. An assessment was conducted to explore material composition and selection (structure–property relations), single and multi-layer coating manufacturing, as well as corrosion environment and testing methods. The aim was to identify the critical areas for research and development in utilizing the feedstock materials and thermal spray coating techniques for applications in molten salt thermochemical applications, as well as use lessons learnt from other application areas (e.g., nuclear reaction vessels, boilers, waste incinerators, and aero engine gas-turbine) where other types of molten salt and temperature are expected. Assessment indicated that very limited sets of coating-substrate system with metallic interlayer is likely to survive high temperature corrosive environment for extended period of testing. However, within the known means and methods, as well as application of advanced thermal spray manufacturing processes could be a way forward to have sustainable coating-substrate assembly with extended lifetime. Spraying multi-layered coating (nano-structured or micro-structured powder materials) along with the application of modern suspension or solution based thermal spray techniques are considered to

This is an open access article under the terms of the [Creative Commons Attribution](https://creativecommons.org/licenses/by/4.0/) License, which permits use, distribution and reproduction in any medium, provided the original work is properly cited.

© 2024 The Author(s). *Engineering Reports* published by John Wiley & Sons Ltd.

result in dense microstructures with improved resistance to high temperature thermochemical environment.

KEYWORDS

electrolysis, hydrogen, thermal spray coatings, thermochemical cycles

1 | INTRODUCTION

Nuclear reactors can serve as a source of high temperature heat for hydrogen production through electrolysis. This heat can be utilized either for generating electricity or facilitating chemical reactions.¹ Considering the temperature range, the water-cooled reactors can produce steam up to 300°C, while gas-cooled reactors can produce process steam up to 540°C, and the high temperature gas-cooled, graphite-moderated reactor (HTGR) can produce process heat up to 950°C.² Furthermore, the electrical power from a nuclear power plant can be used for low temperature water electrolysis (e.g., proton exchange membrane electrolysis or PEME at 20–80°C, alkaline water electrolysis or AWE at 70–90°C). Also, a combination of heat and electrical power can be used for high temperature steam electrolysis (HTSE) or solid oxide water electrolysis (SOWE) at 800–1000°C, whereas heat can be used to split water through thermochemical cycle (for example the iodine-sulfur (I–S) process). There are also hybrid thermochemical processes (e.g., copper-chloride (Cu–Cl), a phase change material or PCM), that use both heat and electricity. In current practice, light water reactors (LWR) which uses normal water as opposed to heavy water can be used for electrolysis, especially using off-peak electrical power. It has also been suggested by Khamis¹ that high temperature gas cooled reactors (HTGR) are an attractive option for electrolysis, including those advanced nuclear reactors such as supercritical water-cooled reactors (SCWR) or very high temperature reactors (VHTR). More generally, the role of nuclear reactors in industrial heat generation has also been assessed.³

Recently the review of Roper⁴ has considered the role of molten salt in energy systems, including generation and storage. Despite of less mature technological aspects, the molten salts have considerable potential in energy applications though some of the technological aspects are less mature. Figure 1 shows a scheme of a molten salt reactor (MSR) nuclear power plant and the location of a thermochemical cycle reactor and high temperature steam for water splitting leading to hydrogen production. In an MSR, the fissile material is dissolved in liquid (molten) salt in the reactor core, where the

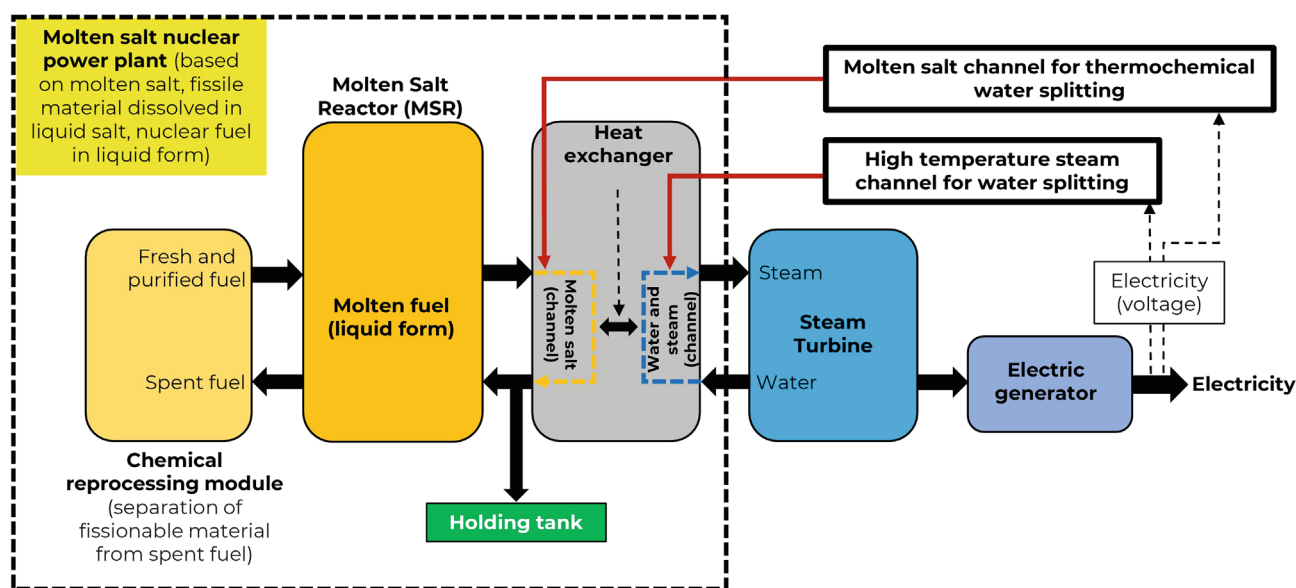


FIGURE 1 Illustration of a molten salt reactor (MSR) nuclear power plant and location of molten salt based thermochemical and steam-based water splitting system for hydrogen production (Authors original image but presented here in simplified form based on reports by Waldrop,⁵ Mallapaty,⁶ and Calderoni and Cabot⁷), attribution is not required to any part of the figure).

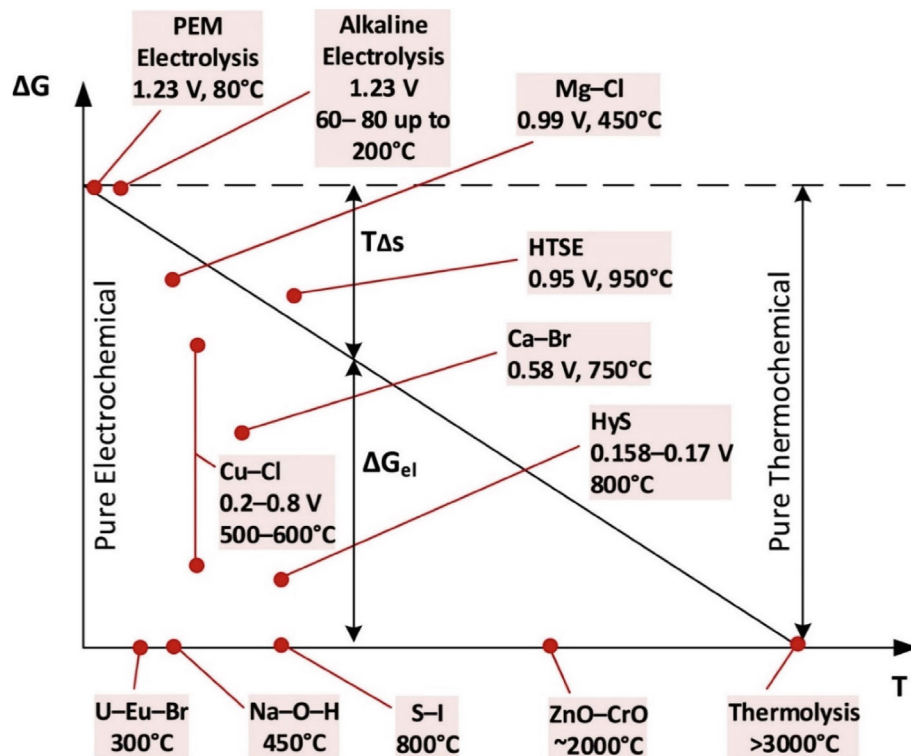


FIGURE 2 Temperatures (T) and theoretical electrical change in Gibbs free energy (ΔG) range and requirements for some hydrogen production methods⁸ (Source: reproduced with permission).

liquid salt also acts as a coolant in place of water.^{5–7} As expected, the nuclear fission occurring in the reactor core generates the heat which are then transferred by the coolant liquid salt and heat exchangers to secondary working fluid (generally supercritical gas) leading to production of high temperature steam and subsequently, the electric generation by driving a turbine. Some part of the heat (thermochemical, steam) and electricity could be used for electrolysis purposes.²

As shown in Figure 2, thermochemical cycles (e.g., Cu–Cl) operate at high temperature, up to 550–600°C.⁸ It also shows that electricity input (i.e., voltage) for electrolysis could be decreased with the increase in temperature. However, high temperature requirements expose the structures to new challenges such as material compatibility and operation durations. Identification and selection of suitable materials is one of the major difficulties facing the development of a thermochemical based hydrogen production plant that can sustain the corrosive and harsh environment for a prolonged use (Figure 3). Current traditional solid-fuel nuclear reactors operate on a 12–18 months cycle of operation (limited by refueling, reactor design and operation duration).⁹ In molten salt reactors (MSRs), the unique design allows for continuous circulation or online refueling to maintain the reactor operation, since the liquid fuel is applied, and in theory, the MSRs could operate on several years depending on the lifespan of graphite. However, the components exposed to molten salts will have to maintain integrity for at least this period before they could be replaced without impacting plant availability.

Coatings of specialized materials have been proposed for such harsh environments.¹⁰ These include superalloys, ceramics, refractory metals, and graphite-based materials, as the most suitable coating materials (on base metal or substrate) for high temperature corrosive environments. Within nuclear context we must also consider radiation. Even if the components are separated from the high intensity neutron radiation in the reactor core, they may be exposed to beta/gamma emitters that can promote chemical reactions through radiolysis such as corrosion. Noteworthy, coating materials can fail due to reasons not related to layer adhesion to substrates, but other factors can be important (Figure 3). These can be geometry of the specimen, factors associated with coating integrity (chemical resistance, thermo-mechanical durability, and surface preparation), as well as failure of equipment that failed to prevent leaking of oxygen, and so on.

This review assesses the possible impact of coating materials used in high temperature corrosive and harsh environment for prolonged duration. This could provide a basis for further research, where the idea could be to develop corrosion-resistant reactors designed for various thermochemical cycles. Following section summarize relevance

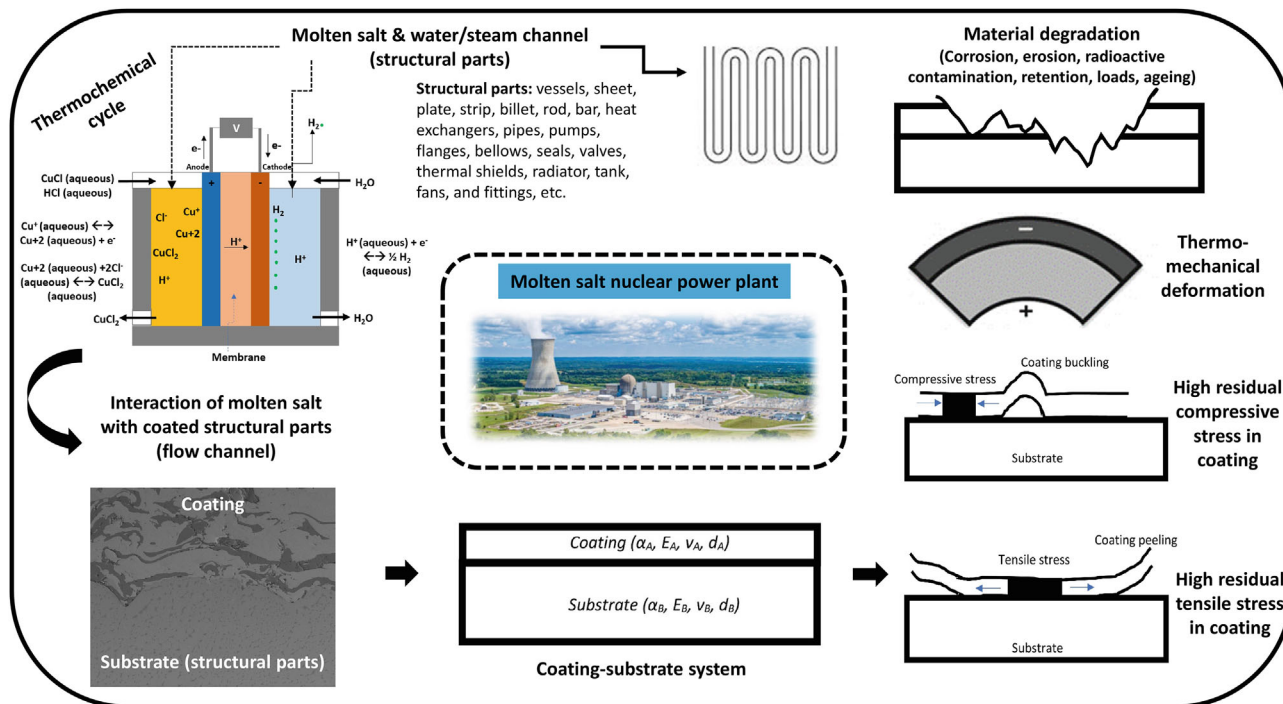


FIGURE 3 Application of heat and electricity sources at nuclear power plant for thermochemical cycle electrolysis and illustration of degradation of coating-substrate system (molten salt channel) (Source: authors original images, attribution is not required to any part of the figure).

of nuclear thermochemical cycles and hydrogen production, presents scarce literature related to thermal spray coatings for molten salt corrosion resistant applications, testing requirements, and then opportunities overview (modeling, radiation-induced damage, and general assessment), and then concluding remarks.

2 | HYDROGEN PRODUCTION AND NUCLEAR THERMOCHEMICAL CYCLES

2.1 | Hydrogen production overview

The recent geopolitical challenges caused a great push towards low carbon hydrogen production technologies to ensure achieving energy security for everyone. Strategic autonomy is vital for most nations, both in terms of energy & industry policy, and this review will address and contribute to the materials and manufacturing strategy ambitions. The global hydrogen energy sector is expected to grow rapidly, with billions of US dollars of investment are being committed by various governments and industry.¹¹ The hydrogen production market size (global) was estimated at USD 158.8 billion (2023), and it is expected to reach USD 257.9 billion, growing at a compound annual growth rate (CAGR) of 10.2% from 2023 to 2028.¹² Within hydrogen production sector, the market of production through electrolysis means is valued at USD 12.9 Billion (in 2023) which is projected to reach USD 25.7 Billion (by 2032), growing at a CAGR of 7.9%.¹³ Overall, there is currently a focus on the deployment of first-generation solutions for nuclear thermochemical cycle electrolysis, as well as planning to scale up the technology to meet short and medium-term targets.¹⁰ There is opportunity for further research and address materials and manufacturing engineering issues in thermochemical cycle electrolysis, as these will be essential enablers in coming decade for further roll-out of hydrogen in energy applications, and this review will address these.

Recent advancement in materials and manufacturing is vital in transitioning towards the cleaner delivery of energy around the world. Hydrogen's promising future as an energy source combined with the possibility of carbonless production results in a highly efficient and attractive alternative to fossil fuels that is predicted to initiate a global demand in the forthcoming decades.¹⁴ Various economies worldwide have introduced a hydrogen-based renewable energy roadmap

which has encouraged the growth of hydrogen-based technologies while setting target deliverables to support the development of hydrogen infrastructure (i.e., production, storage, and usage). As presented in a recent report, the hydrogen generation sector is being driven exponentially up to a predicted 160 billion USD by 2026.¹⁵ Many countries acknowledge nuclear power as a viable low-carbon energy source and has the potential to play a significant role in hydrogen generation in many countries. It is very likely that hydrogen production could play a key role in the global energy system and successfully develop a functioning hydrogen economy.

2.2 | Molten salt and steam interaction with metals

Examples of salt (inorganic) components include BeF_2 , CuCl_2 , MgCl_2 , NaBF_4 and KNO_3 .¹⁶ Molten salts are a phase change material (PCM) that can store and release thermal energy as they change phase (between solid and liquid states). Such materials are solid at room temperature and atmospheric pressure but can change to liquid state when thermal energy is transferred to the storage medium.¹⁷ Due to its liquid form, it can be both the fuel (means it can produce heat) and the coolant (capable of transferring the heat to the power plant). For nuclear reactor applications, a salt mixture (also called as coolant) consists of different components of salt mixed into a multicomponent binary mixture such as LiF-BeF_2 or ternary mixture such as LiF-NaF-KF .¹⁶ Mixing several components into binary or ternary systems reduces the melting point of the resulting salt system to more practical levels. In a molten salt reactor radioactive isotope of nuclear materials (e.g., uranium and thorium) can be dissolved in the molten salt to provide a source of radiogenic heat from a self-sustaining nuclear reaction.¹⁸ It is noted that there are many different types of MSR that have been proposed, with some demonstrated at a small scale.

The original work on the use of molten salts in nuclear energy reactor was carried in 1940's at the Oak Ridge National Laboratory (ORNL). Molten salt reactors operate at high temperatures, leading to increased efficiencies in electricity generation, as well as other high-temperature process heat applications.¹⁹ Electrolysis is one of the most common techniques with a high potential for being integrated with nuclear power to produce low carbon hydrogen through a high-temperature thermochemical cycle.^{20–22} The interaction of molten salt with dissolved nuclear materials in contact with containment vessels and pipes leads to significant corrosion and a range of related problems. Corrosion analysis of containment vessels and pipes still needs research, as it is the least investigated area in the nuclear industry.

2.3 | Corrosive environment in nuclear thermochemical cycles

In thermochemical water splitting process (also called thermolysis or thermal decomposition via high temperature electrolysis (HTE), for example, at nuclear reactors²³), high temperature heat is used to decompose water leading to hydrogen and oxygen production,²⁴ with overall thermal efficiencies of about 50% achievable.²⁵

Various thermochemical cycles such as cerium-iodine (Ce—I) thermochemical cycle,²⁶ iron-chloride (Fe—Cl) thermochemical cycle,²⁷ iodine-sulfur (I—S) thermochemical cycle,²⁸ and copper-chloride (Cu—Cl) thermochemical cycle (Figure 4)^{30–33} for splitting water by using nuclear or in some cases solar heat sources. Since thermochemical cycles operate at high temperatures in a corrosive and harsh environment, the structural components (including electrodes) require special attentions. The accelerated degradation results in an economic problem for the thermochemical cycle operation since the maintenance costs are greatly high. As the temperature of the thermochemical cycle is increased for higher efficiency, the degradation severity of materials is further accelerated. To be able to compete with hydrogen production using other electrolysis methods, more needs to be done in terms of corrosion-resistant materials in thermochemical cycle structural parts. Since corrosion-resistant bulk material (superalloy steel) values (cost) more than a less corrosion-resistant material, that is, low-alloyed steel, therefore, from the economic point of view, an alternative approach could be the application of high-alloyed steel or other materials in the form of a coating on to low-alloyed steel substrate, to increasing the corrosion resistance with good mechanical properties.³⁴

Figure 5 shows a schematic process flow diagram for a Cu—Cl thermochemical cycle. Thermal energy recovery within the Cu—Cl cycle is important step which uses a combination of chemical and electrochemical reactions to separate the water into hydrogen and oxygen. Analysis has shown that around 88% of the recovered heat can be achieved by cooling and solidifying molten copper(I) chloride exiting the oxygen production step of the Cu—Cl cycle.³⁵ Initially, during the reaction between HCl and Cu—Cl, the hydrogen and aqueous CuCl_2 are produced. The aqueous CuCl_2 is then dried to create solid CuCl_2 , which is transferred to a fluidized bed reactor. The heat recovered from the cycle reacts with input water,

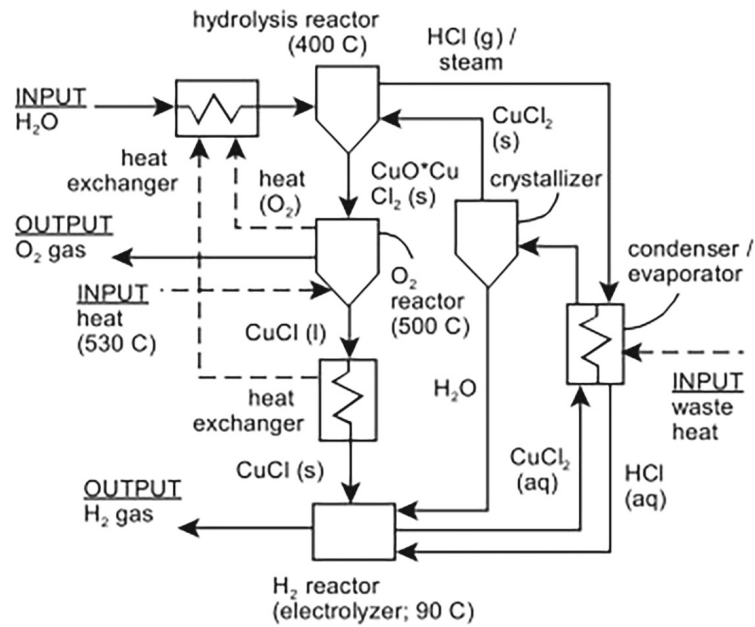


FIGURE 4 Schematic of thermochemical Cu—Cl cycle²⁹ (Source: reproduced with permission).

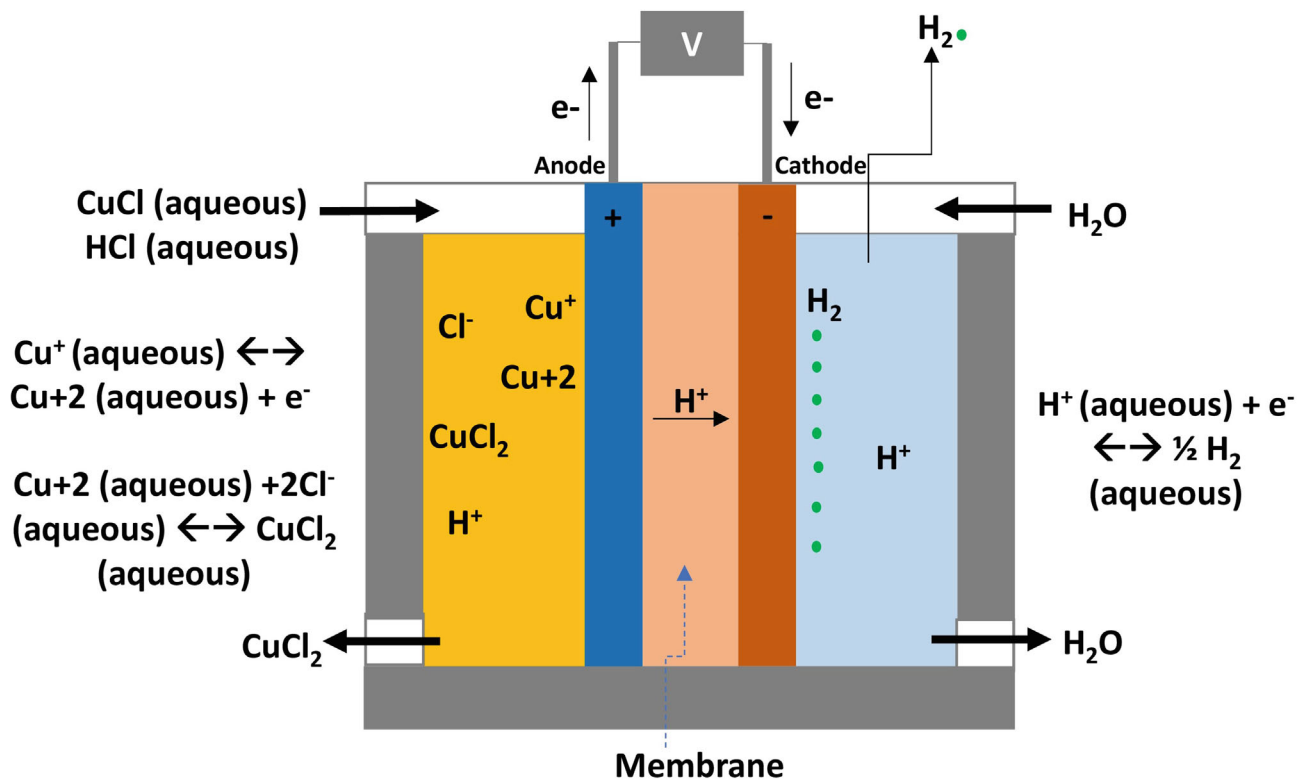


FIGURE 5 Schematic of a molten salt thermochemical water splitting system: Cu—Cl/HCl cycle (authors original image but adapted from Naterer et al.³² (Source: reproduced with permission).

and solid CuCl_2 produces the HCl gas and CuO—CuCl_2 , known as copper oxychloride. The CuO—CuCl_2 is transferred in the molten salt reactor to produce molten Cu—Cl and oxygen.³⁶ Depending on the specific cycle, some common components in nuclear thermochemical cycles include nuclear reactor, heat exchanger, chemical reactors, separation units, recuperator, heat rejection system, and containment structure. Materials selection is crucial for sustainable operation of the thermochemical cycle due to the extreme operating conditions (such as high temperature, radiation exposure, and extremely corrosive environment). Therefore, it is important that the chosen materials exhibit good thermo-mechanical properties, resistance to corrosion, and demonstrate irradiation stability.

2.4 | Structural material selection strategies for thermochemical cycles

Considering thermochemical cycle operating temperature, the choice of materials for structural components is crucial, as the entire system needs to ensure the structural integrity, safety, and efficiency.⁷ At high temperature, the materials should have high mechanical strength to withstand thermal stresses and creep, and the example materials could be high-temperature alloys, refractory metals, and ceramics. Thermal expansion coefficient should be compatible to avoid differential expansion (i.e., between structural parts or substrates and coatings, heat exchangers and insulation layers, and seals and gaskets). To resist high temperature corrosion, resistant to oxidation, and be chemically stable, the materials could be stainless steels, nickel-based alloys, ceramics, and refractory metals. Considering the irradiation stability, the materials (alloys and ceramics) should resist radiation damage such as embrittlement and degradation of mechanical properties. And finally, the cost, access, and manufacturability of materials are also an important consideration which influence the choice of materials. Meanwhile, there is also a need to check the compatibility of the cost-effective salts with the combinations of structural materials (e.g., alloys, graphite, and composites) used in nuclear systems.³⁷

Considering range of factors, the development of innovative and sustainable coatings for key components for structural parts (and electrolyzers) could be a feasible way forward. For the combination of functional reasons (thermo-mechanical, electro-chemical), it is preferred to keep the coated layers thin enough, implying that the reactors are more prone to damage during production, assembly, and operations. Advanced testing and material property characterization are required to optimize the support sections of the layered system (e.g., electrode, electrolyte, and membrane) while maintaining active areas.

The scalability of thermochemical cycle systems (i.e., different scales and applications), can have a notable impact on the material selection for various components. These include size and geometry, manufacturability and its maturity, preferred heat transfer considerations, sustainable materials, materials cost for large and small-scale system, compatibility between materials, design and safety considerations at varying scales, and the regulatory compliance.

2.5 | Potential structural materials for thermochemical cycle

The application of molten salt at high temperature and intense neutron radiation imposes restrictions on the structural part of molten salt reactors that directly interact with the molten salt.³⁸ In a molten salt reactor, main components (or structural parts) that directly/indirectly interacts with the molten salt could be vessels, sheet, plate, strip, billet, rod, bar, heat exchangers, pipes, pumps, flanges, bellows, seals, valves, thermal shields, radiator, tank, fans, and fittings, and so on.

The research conducted in the 1960's at Oak Ridge National Laboratory (ORNL) demonstrated that an Ni-based Hastelloy N (Ni–Mo–Cr–Fe alloy), emerged as the most promising structural material for MSR that utilizes uranium as fuel dissolved in a fluoride salt ($\text{LiF—BeF}_2\text{ZrF}_4\text{—UF}_4$). Its good resistance to corrosion in high-temperature molten salt environment underscores its utility for MSR applications.^{38,39} Apart from Hastelloy N (note: such sector are dominated by trade name, with various percentage composition of elements), other materials investigated for MSR structural applications are stainless steel 304 (Fe–Cr–Ni–Mn–Si alloy), stainless steel 316L (Fe–Cr–Ni–Mo alloy), stainless steel AL6XN (Fe–Ni–Cr–Mo–N alloy), Hastelloy X (Ni–Cr–Fe–Mo alloy), Hastelloy C-276 (Ni–Cr–Mo–W alloy), Inconel 600 (Ni–Cr–Fe alloy), Inconel 617 (Ni–Cr–Co–Mo), Inconel 625 (Ni–Cr–Fe–Mo–Nb–Co alloy), Incoloy 800H (Fe–Ni–Cr alloy), Haynes 230 (Ni–Cr–W–Mo alloy), and Ni-201 (Ni–Fe–Mn–Si alloy), a nearly pure Ni alloy, Nb-1Zr, Mo-30 W, and ferritic martensitic steel JLF-1 (or Fe–9Cr–2W–0.1C), or composites, such as SiC–SiC (i.e., matrix and fiber phase mixed together by various processing methods).^{7,37} Other examples of Ni-based alloys that have been investigated for MSR structural applications include Hastelloy NM, HN80_M-VI, HN80_MTY, HN80_MTW, MONICR, GH3535, EM-721 (note: composition of these alloys not well known).³⁹ It is important to note that Ni-based alloys embrittle when subjected to neutron fluxes

at high-temperature (called neutron embrittlement), which then generate helium (He), which migrates to grain boundaries.⁴⁰ Standards or code qualification (e.g., ASME Boiler and Pressure Vessel Code; Section III: Rules for Construction of Nuclear Facility Components, Division 5: High Temperature Reactors) is necessary for high temperature reactor applications. Currently, there are only five materials approved for use in Division 5: 2 1/4Cr-1Mo and 9Cr-1Mo steels, stainless steel 304, stainless steel 316, and Incoloy 800H, and selective approval for Hastelloy N.³⁹ However, it is important to note that ASME Boiler and Pressure Vessel Code does not address corrosion and radiation damage, but focus on mechanical performance of material (i.e., time and temperature dependency).⁴⁰ To develop a First-of-A-Kind technology demonstrator in relation to thermochemical cycle structural part and electrolyser system, perhaps selective materials (i.e., 2 1/4Cr-1Mo and 9Cr-1Mo steels, stainless steel 304, stainless steel 316, and Incoloy 800H, and Hastelloy N) may be adequate, as such materials are fully code-qualified for nuclear construction if the operating temperature is restricted.

The key challenges for structural materials are corrosion and grain boundary embrittlement leading to surface cracking from the fission product.³⁹ This means a systematic investigation (e.g., elevated temperature tensile strength properties, microstructural stability, weldability, long-time aging and creep rupture, creep-fatigue, MSR salt corrosion resistance, embrittlement resistance and analyzing the radiation effects, thermodynamics simulations of the equilibrium phases) is needed to develop structural materials which could sustain corrosion and grain boundary embrittlement for use in thermochemical cycle electrolysis. The materials degradation of structural parts is a major concern for the industry to meet its commercial viability. Overall, the thermochemical interactions between molten salts and the metallic structures (presence of dissimilar materials) should be evaluated. Such analysis could help determine the degradation and lifetime of the containment materials. There is a need to evaluate corrosivity of molten salt and changing chemical composition of the salt by the neutron flux and any other contamination during operation (e.g., driven by impurities in the molten salt). Eventually, there is a need to have standards or data to support qualification of structural materials for molten salt reactor thermochemical cycle leading to electrolysis and hydrogen production.

As shown previously in Figure 5 (for Cu—Cl/HCl cycle), the thermochemical electrolyser cell structure is composed of catalyst layers (i.e., anode, cathode) and membrane layer (e.g., Nafion/polyaniline and Nafion/polypyrrole composites³¹). During operation, when water is heated to 2000–2500°C, part of which will decompose into monatomic hydrogen, monatomic oxygen, OH, O₂, and H₂.⁴¹ As water decomposes at such high temperature, there could be material and structural stability issues. In addition, sustainable heat sources may not be easily available.⁴² Therefore, usage of chemical reagents has been considered to lower the temperatures, reducing the operating temperature at higher pressures.⁴³ Ceramics, refractory metals, Mo, and Ni-based alloys, graphite-based materials, and Hastelloy C has been the most suitable materials for high-temperature corrosive environments (for Cu—Cl thermochemical cycle).³¹ For such extreme applications, other materials could be considered. For instance, Xie et al.⁴⁴ investigated carbide and nitride materials due to their range of properties, including high hardness, high melting points, and excellent thermal and chemical stability. Wu et al.⁴⁵ investigated mullite materials, due to their high temperature stability, low thermal expansion coefficient, thermal shock resistance, and chemical inertness. Sure et al.⁴⁶ investigated partially stabilized zirconia (PSZ) with graphite coatings, due to improved wear resistance, enhanced lubrication, and thermal stability. Kamali and Fray⁴⁷ investigated graphite, due to combination of temperature resistance, corrosion resistance and mechanical strength. Vignarooban et al.⁴⁸ investigated Hastelloy C276, C-22 and N, Sellers et al.⁴⁹ considered Hastelloy N and Steel 316, due to corrosion resistance in aggressive environments, high temperature stability, and mechanical properties. A comprehensive review about hydrogen production by thermochemical water decomposition method is available elsewhere (e.g., Funk²⁵, O'Brien et al.,⁵⁰ Roeb et al.,⁵¹ Naterer et al.,²⁹ Yadav and Banerjee,⁵² and Naterer et al.³²).

2.6 | Thermal spray coatings for structural parts exposed to molten salt corrosive environment

Considering the focus of this review, this section presents literature related to thermally sprayed coatings for structural parts exposed to aggressive corrosion environment. Thermal spray coating are applied in a wide range of anti-corrosion structural part applications, such as oil and gas, construction, petrochemical, nuclear and marine.^{53,54} There are many thermal spray coating processes,⁵⁵ however, literature indicates that processes used were mainly air plasma spray (APS), high velocity oxy-fuel (HVOF), detonation gun (D-gun), suspension plasma spray (SPS), and solution precursor plasma spray (SPPS) processes.

2.7 | Thermal spray coatings for thermochemical cycle Cu—Cl molten salt corrosion resistant applications

The ambition of the review is to assess the feedstock materials, methods, and protocol in the field of appropriate thermal spray coating manufacturing routes used in the thermochemical cycle molten salt facing structural parts. Some key considerations in selecting a suitable thermal spray coating material for a specific molten salt application involves careful consideration to ensure optimal performance and durability. These includes coating materials which are corrosion resistant and chemically stable, demonstrate high temperature stability and desirable thermal conductivity (to avoid cracking or delamination), high compatibility with the underlying structural parts or substrates (high adhesion strength), dense layer of coating to avoid penetration of corrosive materials, resistant to abrasive particles, ease of coating layer manufacturing, cost effective and environmentally friendly.

There are numerous literatures where thermal spray coating methods have been reviewed and discussed, including conventional as well as some modern methods.^{55,56} However, just to summarize, it is a process where feedstock coating materials (wires, powders, suspension, or solution) are sprayed to form an overlay coating on to a substrate. The sprayed layer is formed on a solid surface by fully or partially melting the feedstock materials in a high temperature zone and propelling the feedstock material towards the solid substrate. It is an agile and scalable deposition technique allowing selective tailoring of microstructure to achieve desired properties, such as microstructure, porosity, density, thickness, and so on. Such coatings have the advantage of providing desirable thickness (from nanometer to millimeter) in an effective manner for engineering materials (e.g., metals, alloys, ceramics, cermets, and polymeric composites). By careful design of thermal spray process, for example, selection of geometry, particle shape and size, crystal structure and arrangement, one can tailor surface properties (including adding corrosion resistant functionality for thermochemical cycle structural parts) without significant surface preparation of the material. If one needs to obtain selective coating properties (including residual strain which is inherent to such thermal spray coatings⁵⁷), there can be many variations possible with functional features aligned to have reduced degradation of coatings.

Though there may be many industrial examples, but very limited studies have been reported (specifically for the Cu—Cl cycle, Table 1) where the application of thermal spray coatings for thermochemical cycle structural parts has been considered at laboratory scale (mainly carried by Canada based researchers such as,^{29,31,32,36,58,59}). Various combination thermal/bond coats and substrates have been studied to determine their behavior at high temperatures molten salt environment. This section presents a performance summary related to selected thermal spray coating and substrate (structural parts) materials.

The lifetime analysis of pipeline structural materials transporting molten Cu—Cl is an important parameter for a thermochemical Cu—Cl hydrogen plant. To investigate this, Siantar³⁶ studied (also reported by Naterer et al.²⁹) on the effect of the molten Cu—Cl immersion test (at 500°C for 100 h) on alloys with high Ni-content with and without surface coatings. Metallic substrates such as Ni-based alloy (e.g., Inconel 625) and super austenitic stainless steel (e.g., AL6XN) were selected to develop corrosion resistance coatings against aggressive molten Cu—Cl exposure. It was suggested that the substrate should possess sufficient inherent corrosion resistance to permit detection of a damaged coating before progressing to catastrophic failure. This strategy could assist in repairing of the coatings instead replacement of the substrates or components. It was also proposed to have a metallic inter-layer coating of Diamalloy (a high nickel-chrome material) as a means of minimizing thermal expansion effects instigated by a brittle coating on a ductile substrate. Therefore, the coatings were a metallic of Diamalloy 4006 and two ceramics of yttria-stabilized zirconia (YSZ) and alumina (Al_2O_3) applied using thermal spray coating methods. Analysis of the sample (i.e., coating-substrate) showed that majority of the deposited layers were damaged and fell-off from the metal substrate. Further analysis showed cracks in the coated samples, indicating the sample geometry could have affected coating integrity. As expected, coating cracking provided a route for the molten Cu—Cl to go underneath the coating, leading to a reaction with the substrate materials. Deposits of copper and iron chloride found on the coating surface indicated that there were corrosion reactions during the immersion test that involved dissolution of metal and reduction of copper. Overall comparison of the coating-substrate structure after immersion test indicated that Inconel 625 substrate was better than stainless steel (AL6XN) substrate, and both Diamalloy 4006 and YSZ ($\text{ZrO}_2\text{-18TiO}_2\text{-10Y}_2\text{O}_3$) coatings provided better protection to the metallic substrate than alumina ($\text{Al}_2\text{O}_3\text{-3TiO}_2$) coating.

Figure 6 shows the sample degradation after immersion tests in Cu—Cl.³² Analysis showed that Diamalloy 4006 with an Al_2O_3 top layer survived for 40 h, whereas a super hard steel (SHS, i.e., iron based super hard steel alloy) coating combination did not survive for 100 h. Analysis showed that Diamalloy coatings performed much better than SHS-9172. Overall, Diamalloy 4006 (high velocity oxy-fuel or HVOF sprayed) was best in the group of tests conducted though with

TABLE 1 Literature examples (thermally sprayed coatings for thermochemical cycle Cu—Cl molten salt applications).

Feedstock materials	Substrate	Thermal spray process	Testing details	Coating degradation related general remarks	References
Ni-based superalloys (Diamalloy 4006)	Ni-based superalloys (Inconel 625)	HVOF	500°C, 100 h, sample in Cu—Cl overnight (8 h), nitrogen flow rate is 20 mL/min. Corrosion test in 0.1 M HCl.	Corrosion behavior of the coating was stable.	36
Ni-based superalloys (Diamalloy 4006) + Alumina (Al ₂ O ₃)	Stainless steel (AL6XN)			Showed better thermal stability. Coating had good adherence with surface and low electrochemical reaction.	36
Ni-based superalloys (Diamalloy 4006) + YSZ	Ni-based superalloys (Inconel 625)			Less reactive and provided good coating stability.	36
YSZ	Ni-based superalloys (Inconel 625)			Nanostructured YSZ coating showed longer lifetime than the conventional coating. Nanostructured YSZ showed high thermal shock resistance.	36
YSZ	Stainless steel (AL6XN)			Loss reactive and showed better stability. Coatings fell off at places while most of the coating remained.	36
Ni-based superalloys (Diamalloy 4006)	Stainless steel (AL6XN)			Coating did not show any significant reaction and degradation. Diamalloy performed much better than the SHS.	36 32
Alumina (Al ₂ O ₃)	Stainless steel (AL6XN)			Coating very reactive and fell off. Low coating stability and adherence.	36
Iron based super hard steel alloy (SHS9172)	Ni-based superalloys (Inconel 625)/Stainless steel (AL6XN)	HVOF, APS	500°C, 100 h (absence of oxygen), argon gas flowrate 110 cc/min	Iron based alloy showed good resistance to corrosion, erosion, and abrasion. Coating failed at high temperature. Presence of the high iron in the coating corroded and decreased the adhesion with the base material.	58

(Continues)

TABLE 1 (Continued)

Feedstock materials	Substrate	Thermal spray process	Testing details	Coating degradation related general remarks	References
SHS	Mild carbon steel		500°C, 50 h (absence of oxygen)	Iron based alloy showed good resistance to corrosion, erosion, and abrasion. Coating lost the stability and fell off. Severe Cu-Cl attack and the coating fell off. The seal did not resolve the porosity issue.	
SHS 9172 + Al ₂ O ₃	Ni-based superalloys (Inconel 625)/Stainless steel (AL6XN)		500°C, 100 h (absence of oxygen), argon gas flowrate 110 cc/min	Iron based alloy showed good resistance to corrosion, erosion, and abrasion. Al ₂ O ₃ showed resistance to corrosion, has high thermal stability, hardness, and wear resistance. High porosity and pore size resulted in reduced mechanical properties of coating and initiate electrochemical reactions. High pore size allowed molten Cu—Cl to react with the base materials and cause corrosion. Different thermal expansion coefficient of the base and coating layers introduced cracks in coating.	
SHS + Al ₂ O ₃	Mild carbon steel		500°C, 50 h (absence of oxygen)	Iron based alloy showed good resistance to corrosion, erosion, and abrasion. Coating lost the stability and fell off. Severe Cu-Cl attack and the coating fell off. The seal did not resolve the porosity issue.	
SHS 9172 + YSZ	Ni-based superalloys (Inconel 625)/Stainless steel (AL6XN)		500°C, 100 h (absence of oxygen), argon gas flowrate 85 cc/min	Iron based alloy showed good resistance to corrosion, erosion, and abrasion. YSZ layer could withstand Cu—Cl environment. In high coating porosity conditions, salt easily penetrates the coating and react with the base material.	

(Continues)

TABLE 1 (Continued)

Feedstock materials	Substrate	Thermal spray process	Testing details	Coating degradation related general remarks	References
Ni-based superalloys (Diamalloy 4006)	Ni-based superalloys (Inconel 625)/Stainless steel (AL6XN)		500°C, 100 h (absence of oxygen), argon gas flowrate 200 cc/min	HVOF spray influenced the hardness and ductility of coating. Low wear resistance. No abnormal attacks on the coating	
Ni-based superalloys (Diamalloy 4006) + Al ₂ O ₃	Ni-based superalloys (Inconel 625)/Stainless steel (AL6XN)	HVOF, APS	500°C, 100 h (absence of oxygen), argon gas flowrate 110 cc/min	<p>Showed better thermal stability.</p> <p>Diamalloy 4006 + Al₂O₃ survived for 40 h. Coating crack on the tip. No large Cu-Cl deposition on the sample.</p> <p>Different thermal coefficient of the coating and base material was the reason for the crack.</p>	32,58
Ni-based superalloys (Diamalloy 4006) + YSZ	Ni-based superalloys (Inconel 625)/Stainless steel (AL6XN)	HVOF, APS	500°C, 100 h (absence of oxygen)	No crack and corrosion observed on the coating layer. Visual examination determined the YSZ layer delamination due to the different thermal expansion of the multilayer coating materials. YSZ coating separated from the bond coating due to high YSZ coating porosity which gives way to Cu—Cl penetration and reaction.	
Ni-based superalloys (Diamalloy 4006) + YSZ	Medium carbon steel	HVOF (Diamalloy), YSZ (APS)	500°C, 48 h	Less reactive and good stability. Localized degradation and delamination and coating showed good adherence. More resistance to Cu—Cl attack. Diamalloy presented good adhesion with base material.	59
YSZ	Medium carbon steel	APS	500°C, 5 h	Severe corrosion of coating. Thin coating layer was not enough to resist the Cu—Cl attack.	

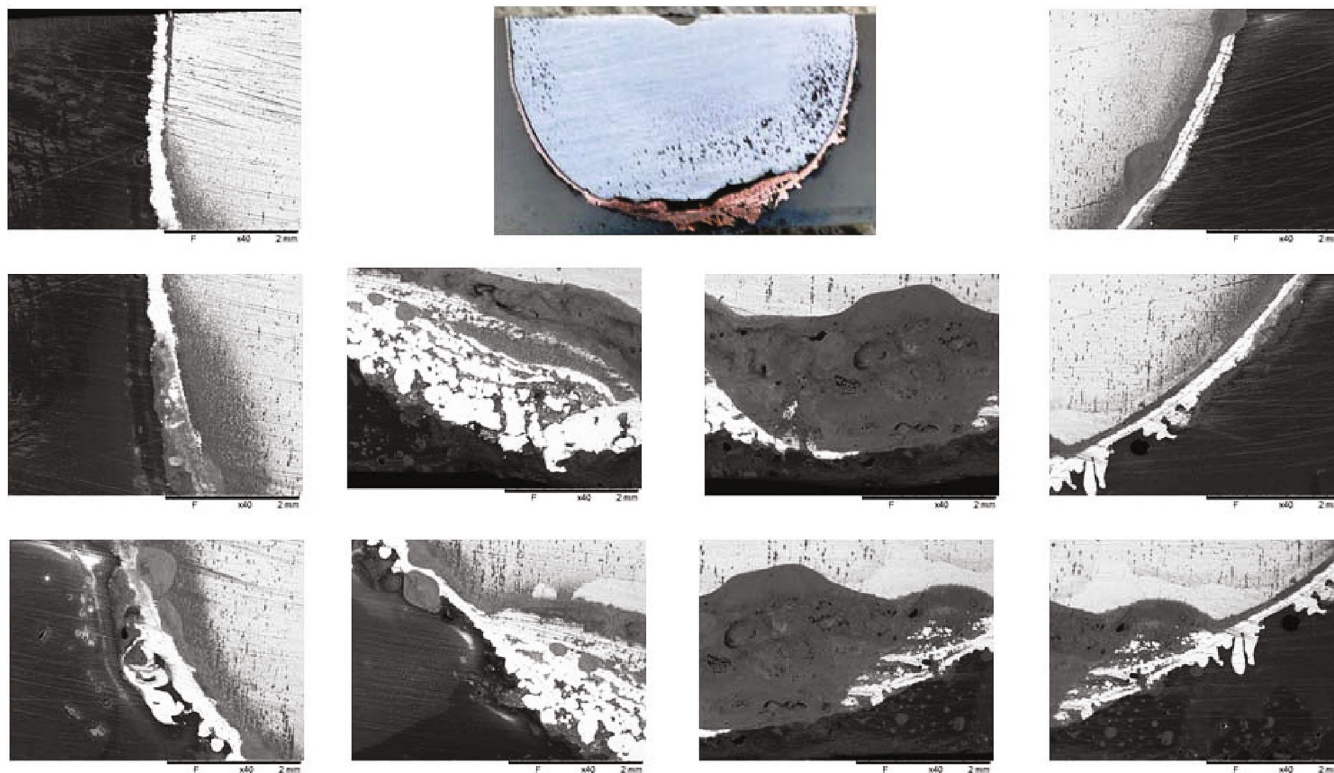


FIGURE 6 Cross-section of high velocity oxy-fuel sprayed diamalloy 4006 showing coating degradation after immersion test in Cu—Cl (each scale bar is 2 mm)³² (Source: reproduced with permission).

damaged tip. Naterer et al.³² suggested that substrates under consideration for future testing should include Ni-based superalloy (e.g., Hastelloy, Udimet 500, IN718, and Nimonic105), and quartz (silica) glass coating.

Azhar⁵⁸ investigated six coating combinations of bond and ceramic coatings for the containment vessels and pipes for thermochemical molten salts environment at high temperature of 500°C, and for 50-h and 100-h test durations. Inconel 625 and super austenitic stainless steel (AL6XN) were considered as substrate metals with thermally sprayed coating materials such as super hard steel (SHS), Diamalloy 4006, YSZ (ZrO₂ 18TiO₂ 10Y₂O₃), and Al₂O₃. Overall results suggested that the combination of Diamalloy 4006 (Diamalloy, Diamalloy+YSZ, Diamalloy+Al₂O₃) performed much better than SHS combination (SHS, SHS + YSZ, SHS + Al₂O₃), as shown in Figure 7. All SHS coatings fell off completely from the substrate. Diamalloy 4006 coatings survived for 100 hours. Corrosion deposits and pure Cu appeared on the samples in most of the cases. Also, it was observed that the Al₂O₃ and YSZ can prevent diffusion of molten salt if these coatings do not crack. Most of the coatings fell off from the substrates during testing and it was suggested that the porosity of the coating layer (in both high velocity oxy-fuel (HVOF) and air plasma sprayed (APS)) should be minimized to protect the underlying coating or substrate materials.

Azarbayjani et al.⁵⁹ investigated thermally sprayed ceramics with metallic coating materials deposited onto medium carbon steel through an immersion test in molten Cu—Cl at 500°C for an extended period. Two types of thermally sprayed coating materials were reported, such as YSZ, Diamalloy 4006 (reported as Ni-20Cr-10W-9Mo-4Cu-1B-1C-1Fe) and YSZ coatings onto steel substrates. It was observed that majority of the coatings were intact and did not fall-off, and that the YSZ coating which was applied to the metallic steel substrate with a bond coating, survived the immersion tests, however it showed corrosion and erosion related degradation within layers, as shown in Figure 8. Azarbayjani et al.⁵⁹ indicated that the primary possible causes of the coating disbonding from the substrate could be the difference between the thermal expansion coefficient of the coating and the substrate, as well as the stress or attached from the molten Cu—Cl. It was suggested that if the crack appears in coating layer, it could provide a pathway for the chemicals to go under the coating layer and react with the base substrate.

As discussed previously through several examples, application of thermal spray-coating processes is successful in strategically developing protective layers against molten Cu—Cl corrosion. It was proposed to manufacture a metallic



FIGURE 7 Examples of immersion tests in Cu—Cl: (i) SHS-9172 specimen; (A) before, (B) after, and (C) after cleaning, (ii) SHS 9172 + Al_2O_3 specimen; (A) before, (B) after, and (C) after cleaning, (iii) SHS-9172 + YSZ specimen; (A) before, (b) after, and (c) after cleaning, (iv) Diamalloy 4006 sample (100 hr test); (A) before, (B) after, and (C) after cleaning, (V) Diamalloy 4006 + Al_2O_3 specimen (100 hr test); (A) after, (b) sample tip after, and (c) specimen with green shades after, (vi) Diamalloy 4006 + YSZ specimen (100 hr test); (A) before, (B) after, (C) sample tip after, and (vii) Diamalloy 4006 + YSZ, Diamalloy 4006 + Al_2O_3 , Diamalloy 4006 specimen (left to right) after the immersion test for 50 hrs (scale bar not available)⁵⁸ (Source: permission obtained ©M.S. Azhar, all rights reserved).

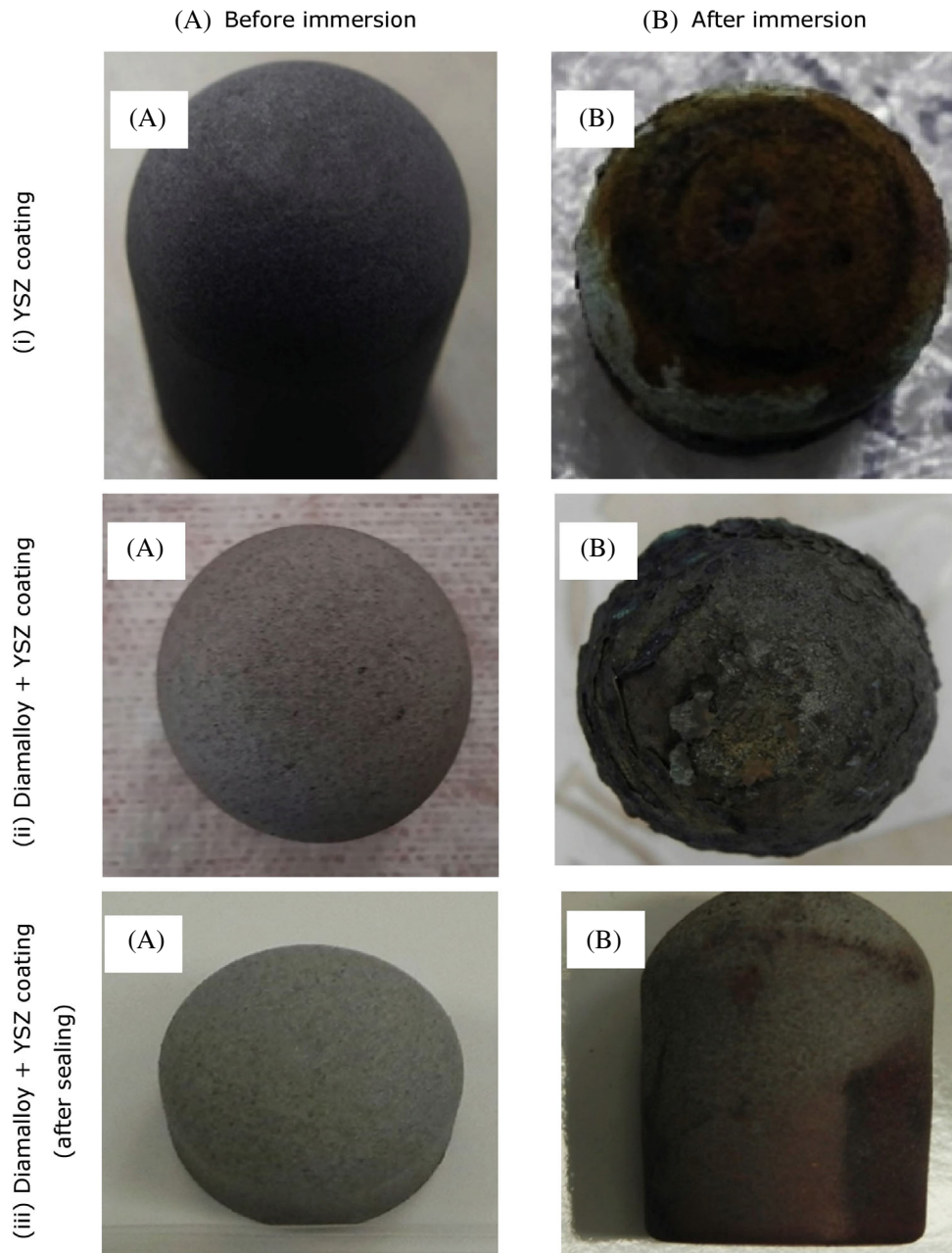


FIGURE 8 Coated specimens (immersion tests in Cu—Cl): (A) before, and (B) after post-immersion cleaning: (i) Ytria-stabilized zirconia (YSZ) coating (after 5 h test), (ii) Diamalloy + YSZ coating (after 48 h test), and (iii) Diamalloy + YSZ coating after sealing (after 100 h test) (scale bar not available)⁵⁹ (Source: reproduced with permission).

inter-layer coating as a means of minimizing thermal expansion and stress effects instigated by overlaid brittle layer on a ductile substrate. Cracks and porosity in the coated top brittle layers are not desirable, as it provides a route for the molten Cu—Cl to go underneath the coating, leading to a reaction with the substrate materials. Various examples of thermally sprayed coatings considered for thermochemical copper—chlorine (Cu—Cl) cycle applications are summarized in Table 1.

2.8 | Thermal spray coatings for other molten salt corrosion resistant applications

Corrosion-resistant coatings play a crucial role in protecting components from the damaging effects of a corrosive environment. Depending on the corrosive environment there are examples where several thermal spray coatings have been

studied.⁶⁰ Some of the know-how (mainly those related to aggressive corrosive resistant applications, other than those tested in Cu—Cl molten salt environment summarized previously), and new design of thermal spray coatings could be useful for thermochemical cycle electrolysis applications. The example applications discussed here include thermal spray coating when tested in aggressive corrosive environment at high temperature, such as nuclear reaction vessels, boilers, waste incinerators, aero engine gas-turbine, and so on. The nuclear reactors are nuclear power plants components where controlled nuclear reactions take place to produce heat.⁶¹ The boiler systems at power plants operate at high temperature, pressure, and chemically aggressive environments, leading to corrosion related degradation and failure.^{62–64} Waste incinerators operate under harsh conditions, with high temperatures, corrosive gases, and abrasive particles, and are used to burn solid waste at high temperatures, converting it into ash, gas, and heat.^{65,66} Examples related to thermal barrier coatings of aero engines are included here as such components typically withstand the high temperature and gas pressure, as well as corrosion and erosion.⁶⁷ As follows, there are multiple lessons related to materials degradation which could be relevant for thermochemical cycle applications.

For pyrochemical reprocessing plant applications (i.e., nuclear fuel recycling process or salt purification vessel), Shankar et al.⁶⁸ investigated APS sprayed 8 wt.% YSZ (composition: Y_2O_3 (7–9 wt%)– SiO_2 (1 wt%)– TiO_2 (0.2 wt%)– Al_2O_3 (0.2 wt%)– Fe_2O_3 (0.2 wt%)– ZrO_2 (balance)) coatings deposited onto vacuum plasma sprayed (VPS) NiCrAlY metallic bond coat with stainless steel 316 L substrate. The corrosion tests were carried out in molten chloride salt (i.e., LiCl–KCl) at 600°C for 5 h, 100 h, and 500 h. Overall analysis indicated that the coatings did not show significant degradation under corrosion attack (Figure 9i). To consolidate the coatings, laser melting using a CO_2 laser of the coated samples was carried which led to the development of large grains of zirconia (and eliminated porosity) with segmented cracks (due to shrinkage and relief of thermal stresses). It was also noticed that laser melting led to the elimination of coating defects and showed smooth surface (Figure 9ii).

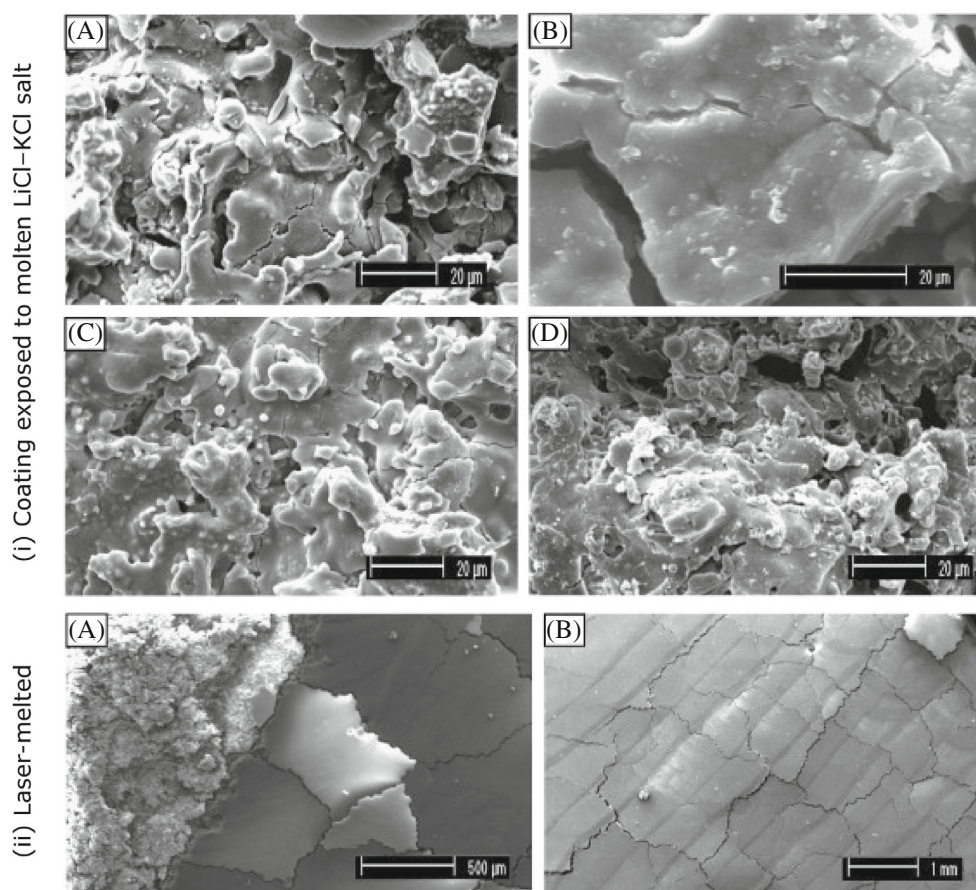


FIGURE 9 Microscopic images of APS sprayed partially stabilized (~8 wt.%) zirconia coating surface: (i) (A) as-coated, (B) 5 h exposed, (C) 100 h exposed, and (D) 500 h exposed to LiCl–KCl molten salt, and (ii) laser-melted surface at (A) 50 W, and (B) 100 W⁶⁸ (Source: reproduced with permission).

For nuclear waste management and related electrochemical reduction process components (e.g., reaction vessels, electrodes, and other metallic components), Lee and Baik⁶⁹ developed APS sprayed coatings, that is, Al_2O_3 and 8 wt.% YSZ coatings onto CoNiCrAlY bond coat with Ni-alloy (Inconel 713LC) substrate. The investigation was for the purpose that coated parts must endure hot corrosion environment and remain resistant. The corrosion tests of coatings were carried out in LiCl-3 wt.% Li_2O molten salt at 650°C under an oxidizing environment for 24–168 h test duration. Corrosion analysis showed that the Al_2O_3 coating reacted with LiCl-3 wt.% Li_2O molten salt forming a reaction layer (porous) of LiAl, Li_5AlO_4 and LiAl_5O_8 , whereas the YSZ coating formed non-crystalline phase dense reaction layer and offered a better protection as well as effective barrier against the molten salt. Further analysis showed that the molten salt penetrated through to the coating pore and reaction products were formed at the intra-pores and splat boundaries. Such penetration of molten salt is possible in coatings which typically contain various types of defects, for example, incompletely filled pores, inter-splat pores and intra-splat space or microcracks.

For molten salt fast reactor (MSFR) applications, Brupbacher et al. (Brupbacher et al 2015) investigated binder-free chromium carbide (Cr_3C_2) coatings which was deposited on to Ni-based alloy (H230) (Ni–Cr–W system) substrate using air plasma spray and cold spray techniques. This coating was developed for potential test in molten fluoride salt; however, it was found to be not suitable for application requiring molten fluoride salt corrosion resistance. The emergence of porosity in the coatings during processing may not be favorable for the proposed applications.

For biofuel-fired boiler (superheaters) applications, Uusitalo et al.⁷⁰ investigated HVOF sprayed Ni–49Cr2Si, Ni–57CrMoSiB, Ni–21Cr9MoFe, Fe–15Al–2Cr, and Ni–50Cr coatings deposited on to steel substrates. The corrosion tests were carried at 550°C (for 100 h duration) below a synthetic salt deposit (salt was partially molten in the order of 50% at 550°C). During corrosion test, the test samples were covered with salt (40 Na_2SO_4 , 40 K_2SO_4 , 10 NaCl , and 10 KCl) which were then exposed to oxidizing (N_2 –20 H_2O –14 CO_2 –3 O_2 –500 ppm HCl) and reducing (N_2 –20 H_2O –5 CO –0.06 H_2S –500 ppm HCl) environment the corrosion of coating in presence of salt during combustion of chlorine containing nuclear fuels. Analysis showed that the deposited coatings were susceptible to chlorine attack in both oxidizing and reducing atmosphere through interconnected oxide network at splat boundaries within coatings (Figure 10i). During oxidizing conditions, the Ni–57CrMoSiB coating performed well forming protective layer of oxide, whereas all the other coatings formed only non-protective layers. Overall, it was suggested that the interconnected coating porosity, oxide-containing splat boundaries, and compositional inhomogeneities could limit the corrosion resistance of coatings. Uusitalo et al.⁷⁰ suggested that if oxidation of coatings takes place (along with presence of voids at splat boundaries), then chlorine circulating through the coatings may cause significant damage and degradation of coatings and could affect the strength of interfacial bonding between the substrate and coatings. It was also suggested that if the chlorine compound transport through coating layers is slow, the coatings could hold their capability to protect the underlying substrates.

For boiler applications (superheater and re-heater materials), Sidhu et al.⁷² investigated high temperature corrosion behavior of HVOF sprayed Cr_3C_2 –NiCr, NiCrBSi, Stellite-6, and Ni–20Cr coatings deposited on to Ni-based superalloy (i.e., Superni 75 or 19.5Cr–3Fe–0.3Ti–0.1C–balance Ni). Testing and analysis in a corrosive environment of condensed alkali molten metal salt Na_2SO_4 –60% V_2O_5 at 900°C under cyclic conditions showed that all coatings were superior to bare substrate. Note about molten metal salt [Na_2SO_4 , V_2O_5 , $\text{Fe}_2(\text{SO}_4)_3$]: the residual fuel oil contains Na, Va, and S as impurities which reacts together to form ash at high temperature (approximately 700–900°C), and which deposit on the material and cause hot corrosion Sidhu et al.⁷² The Ni–20Cr coated sample demonstrated high temperature corrosion resistance with negligible spalling, whereas the Stellite-6 coated samples indicated minimum high temperature corrosion resistance with marginal spalling (note: high temperature corrosion resistance of Cr_3C_2 –NiCr coating was slightly better than NiCrBSi coating). The formation of oxides along the splat boundaries and spinels of Ni, Cr or Co were the reason to have hot corrosion resistance of all coatings. Similarly, Singh et al.⁷³ compared the performance of Cr_3C_2 –25(Ni–20Cr) and Ni–20Cr coatings sprayed on to T91 boiler tube steel using HVOF and tested at 900°C under cyclic conditions. The results showed that the uncoated steel tube experienced higher weight gain (due to the formation of Fe_2O_3 oxides), and the Ni–20Cr coating was less protective compared to Cr_3C_2 –25(Ni–20Cr) coating.

For range of applications (e.g., boiler, internal combustion engine, gas-turbines, fluidized bed combustion, and industrial waste incinerators), Chatha et al.⁷¹ investigated HVOF sprayed 80Ni–20Cr and 75 Cr_3C_2 –25(Ni–20Cr) coatings deposited on to T91 boiler tube steel. The samples were exposed to Na_2SO_4 –60% V_2O_5 molten salt at 750°C under cyclic conditions. Analysis showed that oxide scale phases of the coated samples were mainly oxides and spinels of Ni and Cr (which is protective against the hot corrosion), and that the 80Ni–20Cr coating showed more protective features than the 75 Cr_3C_2 –25(Ni–20Cr) coating. Considering the degradation of both coatings, perpendicular cracks in the coatings were observed (Figure 10ii, iii). Such vertical cracks were attributed to thermal expansion mismatch between the coatings and substrate, and uneven thermal shock.

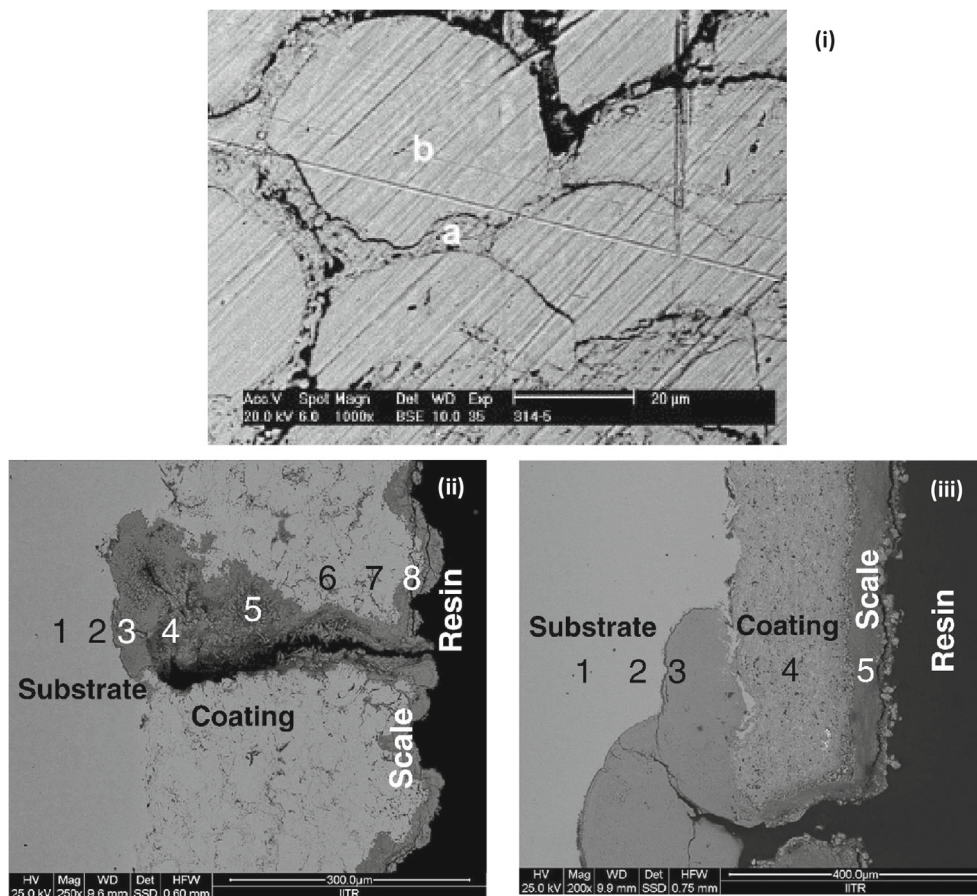


FIGURE 10 High velocity oxy-fuel thermal sprayed coating cross-sections: (i) Ni-21Cr9Mo coating after exposure in oxidizing ($N_2-20H_2O-14CO_2-3O_2-500$ vppm HCl) atmosphere, where the splat boundaries were attacked by chlorine (A is labeled as splat boundaries, B is labeled as composition of the splats which remained unaffected,⁷⁰ (ii) 80Ni-20Cr coating, and (iii) 75Cr₃C₂-25(Ni-20Cr) coating (both coating subjected to the cyclic oxidation in Na₂SO₄-60%V₂O₅ environment at 750°C for 50 cycles)⁷¹ (Source: reproduced with permission).

For biomass incinerator applications, Paul and Harvey⁷⁴ investigated HVOF sprayed coatings (NiCrBSiFe, alloy 718, alloy 625, and alloy C-276) deposited on to P91 substrates. The corrosion testing of coated samples was carried at ~525, 625, and 725°C in K₂SO₄-KCl mixture and gaseous HCl-H₂O-O₂ containing environments. Analysis of corroded samples showed that at 725°C, the alloy 625, alloy 718, and NiCrBSiFe coatings performed better than alloy C-276 coating. Considering the corrosion mechanism, it was suggested that in such coatings, the inter-splat boundaries form the weakest part and that is where corrosion initiates. Further on, once the corrosion initiates at the splat boundaries and corrosion product forms, mechanical stresses are generated at the interface, causing blistering, and peeling of the corrosion layer. And, as schematically illustrated in Figure 11, in cases where an oxide layer is formed (forming a protective layer), spalling of the top layer could be mitigated, however when exposed to molten salt and HCl-containing environments, corrosive gases could penetrate through the inter-connected/inter-splat porosity, leading to accelerated corrosion rate and significant degradation of coating-substrate system.

For boiler applications, Oksa et al.⁷⁵ investigated high temperature molten salt corrosion behavior of HVOF sprayed coatings (i.e., nickel-based alloys with high chromium content NiCr, IN625, and Ni-21Cr-10W-9Mo-4Cu or Diamalloy 4006, and iron-based Fe-25Cr-15W-12Nb-6Mo or SHS9172). The coatings were deposited onto X20CrMoV121 (X20), Nimonic® alloy 263 (Alloy 263) and iron-based alloy (Sanicro 25) substrates. The corrosion tests were carried in a molten alkali chloride salt (NaCl, KCl, and Na₂SO₄) at 575°C and 625°C. Results demonstrated that Diamalloy 4006 coating and SHS9172 coating had the best corrosion properties, however, vertical cracking in SHS9172 coating were observed, potentially due to combined effect of corrosion and high tensile residual stresses in coatings. The NiCr and IN625 coatings protected the substrates but formed thick corrosion deposits when tested at 575°C.

For boiler applications, Mishra et al.⁷⁶ investigated Stellite-6 (C-1.05, W-4.48, Ni-1.95, Fe-1.78, Cr29.50, Si-1.18, Mg-0.45, Co-balance) and Stellite-21 (C-0.25, Mo5.5, Ni-3.0, Fe-1.0, Cr-29.0, Si-1.0, Co-balance) coatings deposited by

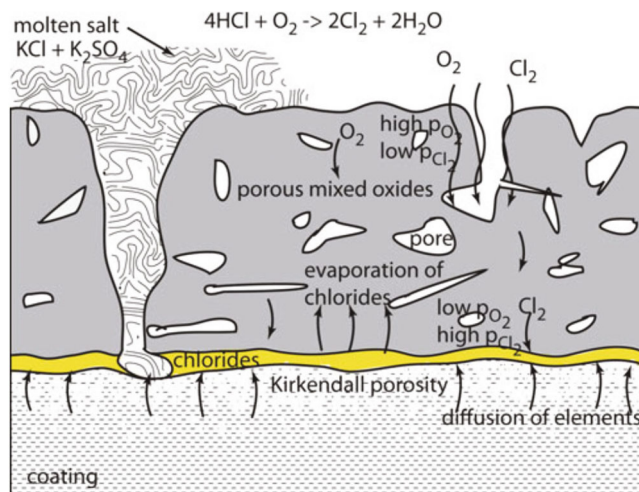


FIGURE 11 Corrosion mechanism at high temperature (with cases where oxide layer forms)⁷⁴ (Source: reproduced with permission).

detonation gun method on to boiler steel SAE 431 substrate (i.e., C-0.16, Mg-1.0, Si-1, S-0.03, P-0.04, Cr-16, Ni-2.5, and Fe-balance). The hot corrosion performance was carried in an aggressive environment of Na₂SO₄-82%Fe₂(SO₄)₃ under cyclic conditions at an elevated temperature of 900°C. The overall comparison showed that Stellite-6 coating had a better hot corrosion resistance than Stellite-21 coating, due to Stellite-6 coating's characteristics of forming a diffusion barrier layer to the degrading species through formation of chromium oxides. The microcracks which originated from the edge of the Stellite-21 coated sample led to coating spallation and higher weight loss.

For applications related to garbage incinerator and boiler tubes, Porcayo-Calderón et al.⁷⁷ investigated hot corrosion behavior of Ni20Cr coatings which deposited on to stainless steel 304 by HVOF method. The samples were tested in ZnCl₂-KCl molten salts 350, 400, and 450°C. At the highest temperature of 450°C, there was some degradation of the coating surface, leading to molten salt penetration slightly into the coating. However, overall analysis showed that Ni20Cr coatings had higher corrosion resistance in ZnCl₂-KCl molten salt at all temperatures than 304 stainless steel substrates. While Cr and Fe played a detrimental role, it was implied that a high Ni content (or Ni-rich coatings) was effective in improving the corrosion resistance.

For applications related to boiler tubes, Oksa et al.⁷⁵ investigated multiple HVOF sprayed coatings (NiCr (Ni-980-1/1260F), IN625 (Diamlloy 1005), Ni-21Cr-10W-9Mo-4Cu (Diamalloy 4006), and Fe-25Cr-15W-12Nb-6Mo or SHS9172 (SHS 9172HV1)) deposited on to stainless steel substrates. High temperature corrosion tests were carried out in NaCl-KCl-Na₂SO₄ salt (which transforms in the molten state) with a controlled H₂O atmosphere at 575°C and 625°C. Analysis showed that the Diamalloy 4006 and SHS9172 coatings had the best corrosion properties against molten salt attack. While the NiCr and IN625 coatings were able to protect the substrates but formed thick layers of corrosion deposits. Overall, it was suggested that coatings with low porosity (HVOF offers dense coatings) and high lamellar cohesion is necessary, as the lamellar boundaries act as corrosion paths, and any detachment of the lamellas could lead to coatings degradation in molten salt corrosion conditions.

Liu et al.⁷⁸ investigated APS 8 mol.% Sc₂O₃, 0.6 mol.% Y₂O₃-stabilized ZrO₂ (i.e., ScYSZ) thermal barrier coatings deposited on to Ni-25Co-20Cr-8Al-4Ta-0.6Y (wt.%) bond coat which was deposited on to nickel-based (IC 10) superalloys. The corrosion tests were carried out in Na₂SO₄ (99.5%) + V₂O₅ (99.9%) salt at 1000°C. Analysis showed that the ScYSZ coating had better chemical and phase stability compared to traditional YSZ coating (Figure 12). However, the destabilization of ScYSZ coating was attributed to the deficiency of stabilizers which resulted from the synergic mineralization effect of vanadium-containing compounds. It was found that the phase transformation (from tetragonal-to-monoclinic) of ZrO₂ could induce the cracks in ScYSZ coating, which is responsible for the degradation of the thermal barrier coatings.

For coal-fired gas-turbine applications, Kamal et al.⁷⁹ investigated detonation-gun sprayed Cr₃C₂-NiCr coatings deposited on to Ni-based superalloys (superni 75, superni 718, Fe-based superalloy superfer 800H). The cyclic hot-corrosion studies were carried out in 75 wt.% Na₂SO₄ + 25 wt.% K₂SO₄ molten salt at 900°C for 100 cycles. Analysis showed that Cr₃C₂-NiCr-coated sample had better hot-corrosion resistance than the uncoated substrates. This was due to the formation of crack free protective oxides (i.e., Cr₂O₃, NiO and formation of their spinel NiCr₂O₄ via solid phase

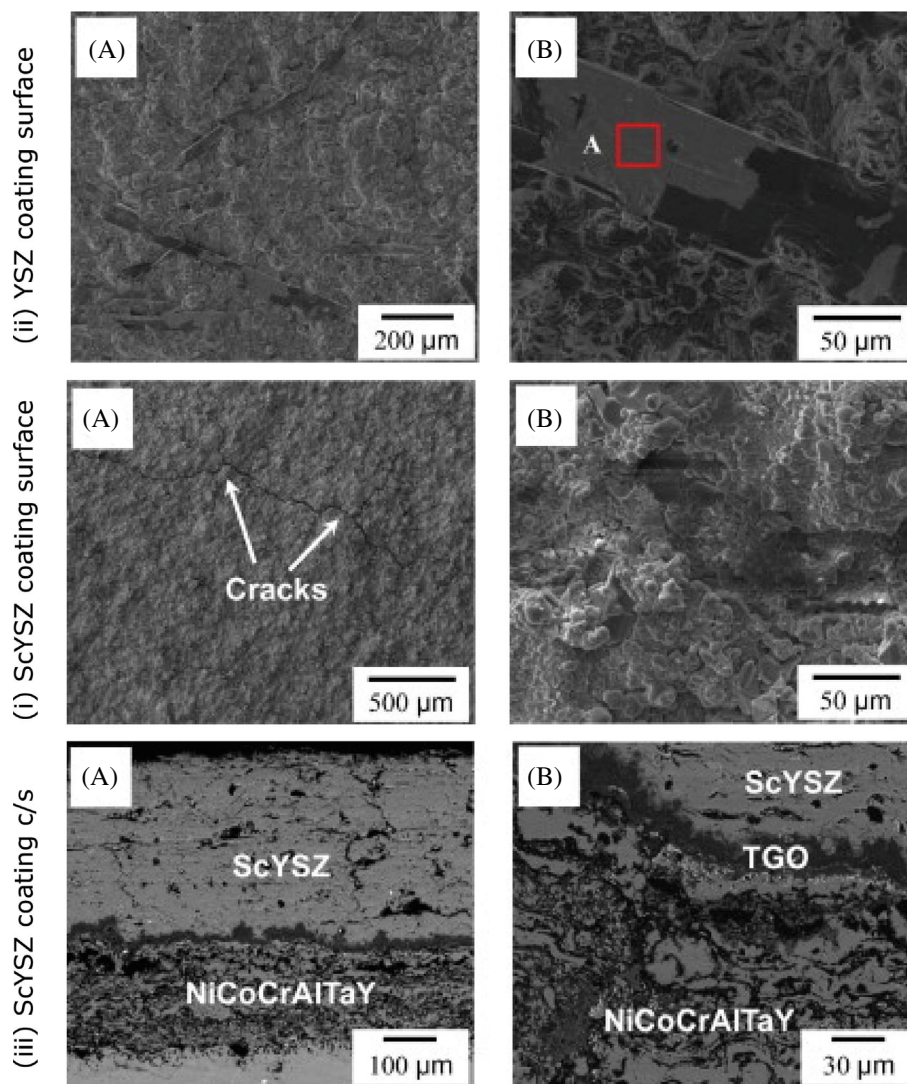


FIGURE 12 Microscopic images of APS coating after 100 h corrosion in $\text{Na}_2\text{SO}_4 + \text{V}_2\text{O}_5$ molten salt: (i) yttria-stabilized zirconia (YSZ) coating surface: (A) and (B) surface morphologies showing large plate-like crystals, (ii) ScYSZ coating surface: (A) surface morphologies with no corrosion product on the corroded surface, (B) coating surface exhibiting a significant difference, and (iii) (A) coating cross-section showing impenetrable vertical cracks formed in ScYSZ (resulted from the phase transformation of t' - ZrO_2 and creation of stress), and (B) TGO layer formed between the ScYSZ coating and bond coating⁷⁸ (Source: reproduced with permission).

reaction), which leads to a slow oxide scale growth, blocks pores, and acts as diffusion barriers to the inward diffusion of corrosive species.

Loghman-Estarki et al.⁸⁰ investigated corrosion resistance of APS sprayed duplex thermal barrier coatings, that is, scandia and yttria co-doped zirconia (nano-4 mol%SYSZ and micro-8.6SYSZ) and yttria doped zirconia (4YSZ) topcoat deposited on to NiCrAlY bond coat with Ni-based super-alloy (i.e., Inconel 738, Ni-15Cr-8.5Co) substrate. The corrosion tests were carried out in 25 mg molten vanadium oxide (V_2O_5) salt at 910°C for different times. Nanostructured coating (4SYSZ) showed a higher corrosion related degradation resistance. The resistance was due to increased compliance capabilities which resulted from the extra porosity presence associated with the nano-zones, including high surface roughness and fracture toughness. Factors associated with the degradation in coatings included destroying splat features (loose coral-like regions), formation of destructive crystals, stresses resulting from thicker thermally grown oxide (TGO), and phase transformation.

For thermal barrier gas-turbine coating applications, Jonnalagadda et al.⁸¹ investigated the attack of vanadium pentaoxides (V_2O_5) or sodium sulphate (Na_2SO_4) on the suspension plasma sprayed (SPS) yttria-stabilized zirconia (YSZ) and gadolinium zirconate (GZ)/YSZ coatings, deposited onto Hastelloy-X substrate with Co32Ni17Cr8Al0.5Y (AMDRY

9951) bond coat. The corrosion tests were carried at 900°C for 8 h. Analysis showed that molten salts infiltrate the coating through micro-cracks and pores, causing leaching of yttria from YSZ. The leaching of yttria destabilizes YSZ, led to an undesired phase transformation of zirconia from tetragonal to monoclinic, which damaged the coating. Additionally, stress was associated with YVO_4 formation, contributing to overall corrosion damage. Conversely, in the presence of gadolinium zirconate (GZ), a low-reactive topcoat material, the columnar boundaries acted as active pathways for molten salts, enabling extensive salt infiltration. As a result, the corrosive product $GdVO_4$ formed between the columns, as shown in Figure 13. The presence of such corrosion products can reduce strain tolerance and cause cracking in SPS coatings.

For thermal barrier gas-turbine coating applications, Hajizadeh-Oghaz et al.⁸² investigated hot corrosion behavior of APS ceria–yttria co-stabilized zirconia (CYSZ) nanostructured coatings ($ZrO_2-2.5 \text{ wt}\%Y_2O_3-25 \text{ wt}\%CeO_2$) deposited on to Amdry 962 (Ni22Cr10Al1Y) bond coat with Inconel 738 (Ni–15Cr–8.5Co) as substrate. The corrosion was carried in molten salt (45 wt.% $Na_2SO_4 + 55 \text{ wt}\%V_2O_5$) for 6, 12, 18, 30, 72, 156, and 300 h at 1000°C. Analysis showed that CYSZ (nanostructured) thermal barrier coatings exhibited superior hot corrosion resistance compared to YSZ and CYSZ (both conventional) thermal barrier coatings. Reasons were attributed to the robust acidity and high content of the stabilizer (when compared with YSZ), and the resistance of molten salt to diffuse in nanoporous CYSZ microstructures. However, the creation of ZrO_2 and YVO_4 , $CeVO_4$, and $Ce_{0.75}O_2Zr_{0.25}$ crystals (all hot corrosion products) on the exterior topcoat CYSZ surface led to the formation of tensile stress which then led to delamination and cracking of exterior or top part of coatings (Figure 14).

For calcia-magnesia-alumino-silicate ($CaO-MgO-Al_2O_3-SiO_2$ or CMAS) resistant thermal barrier gas-turbine coating applications, Fan et al.⁸³ investigated supersonic atmospheric plasma sprayed (S-APS) YSZ and ScYSZ coatings deposited onto aluminium substrate. Through investigation (i.e., TBCs and CMAS interactions in a muffle furnace carried at 1320°C for 24 h and 72 h, that is, a high-temperature furnace which typically involve combination of materials testing, heat treatment, and ashing), it was observed that even though the dense and bulk YSZ material still cannot prevent the infiltration of CMAS, the effect of defects on the CMAS infiltration of the YSZ coating is limited. Overall, it was demonstrated that the addition of Sc_2O_3 could improve CMAS resistance of the YSZ coating, due to lesser solubility of Sc^{3+} (compared to Y^{3+}) in the CMAS, and that it is not easy to form *m*-phase, indicating that the ScYSZ has higher *t*-phase stability under CMAS attack than that of conventional YSZ.

In a recent work for the application related to thermal barrier for gas-turbine coating, Praveen et al.⁸⁴ develop hybrid double-layered TBCs (solution precursor plasma sprayed lanthanum zirconate (LZ), and pyrochlore-fluorite cerium doped lanthanum zirconate (LZC) + air plasma sprayed YSZ) and evaluated high temperature corrosion behavior of the coatings in $Na_2SO_4 + V_2O_5$ environments at 800°C. It was proposed that solution precursor plasma spraying (SPPS), which is a promising thermal spray technique which could develop thin layer with precise control over the composition and stoichiometry of the coating, fine-porosity, phase pure and vertically cracked LZ, and LZC coatings over APS sprayed YSZ layer to produce hybrid double-layered thermal barrier coatings (TBCs) (Figure 15). Analysis showed that the corrosive salt interaction with YSZ coatings resulted in primary corrosive product (i.e., YVO_4) along with monoclinic phase transformation, potentially due to temperature and chemical composition changes, leading to structural change (volume

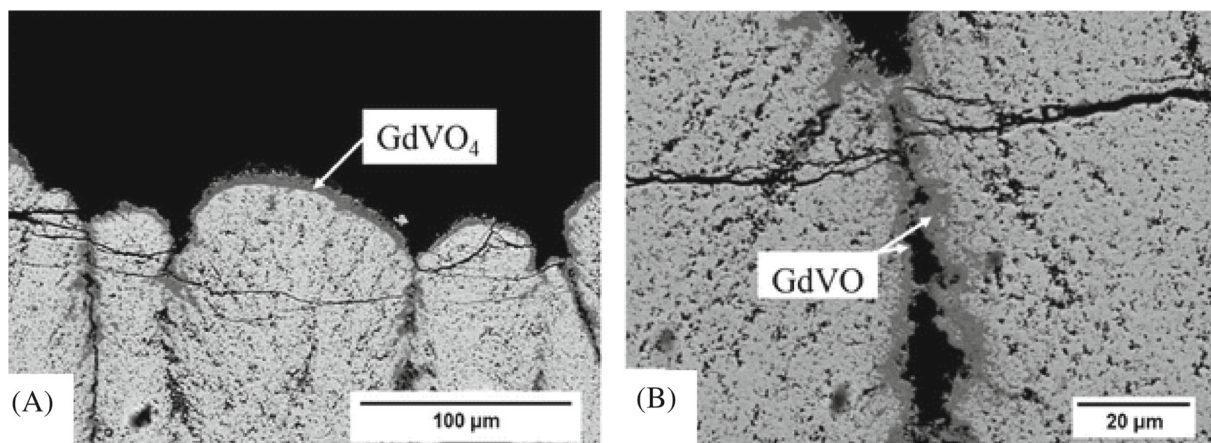


FIGURE 13 Cross section of two-layer gadolinium zirconate SPS coatings: (A) $GdVO_4$ on the top surface, and (B) $GdVO_4$ formation between the columns⁸¹ (Source: reproduced under the terms of the Creative Commons CC BY license).

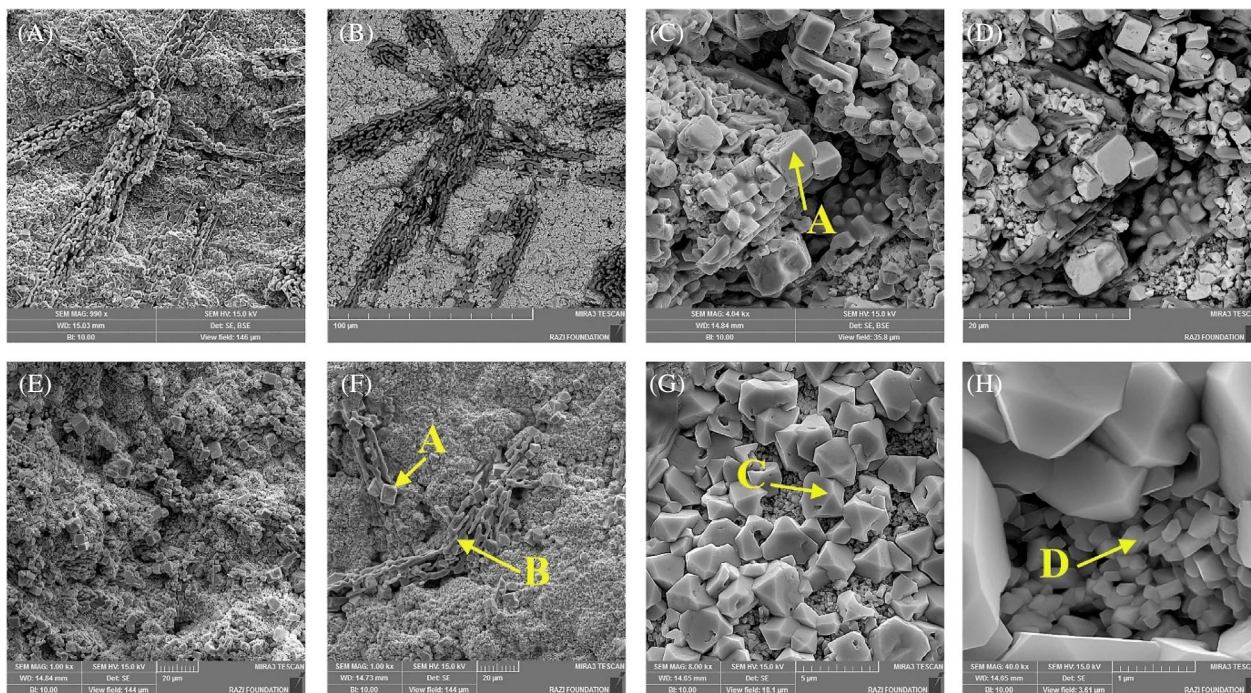


FIGURE 14 Microscopic images of top surface of CYSZ nanostructured APS coatings after toleration of hot corrosion carried in molten salt (45 wt.% Na_2SO_4 + 55 wt.% V_2O_5) for 300 h (presence of cerium, oxygen, zirconium, yttrium, and vanadium was shown at the cubic-like crystals A and C, semi-rod crystals B were composed of cerium, yttrium, oxygen, vanadium, and minor zirconium, and D showed only the presence of cerium, oxygen, zirconium, and yttrium elements)⁸² (Source: reproduced with permission).

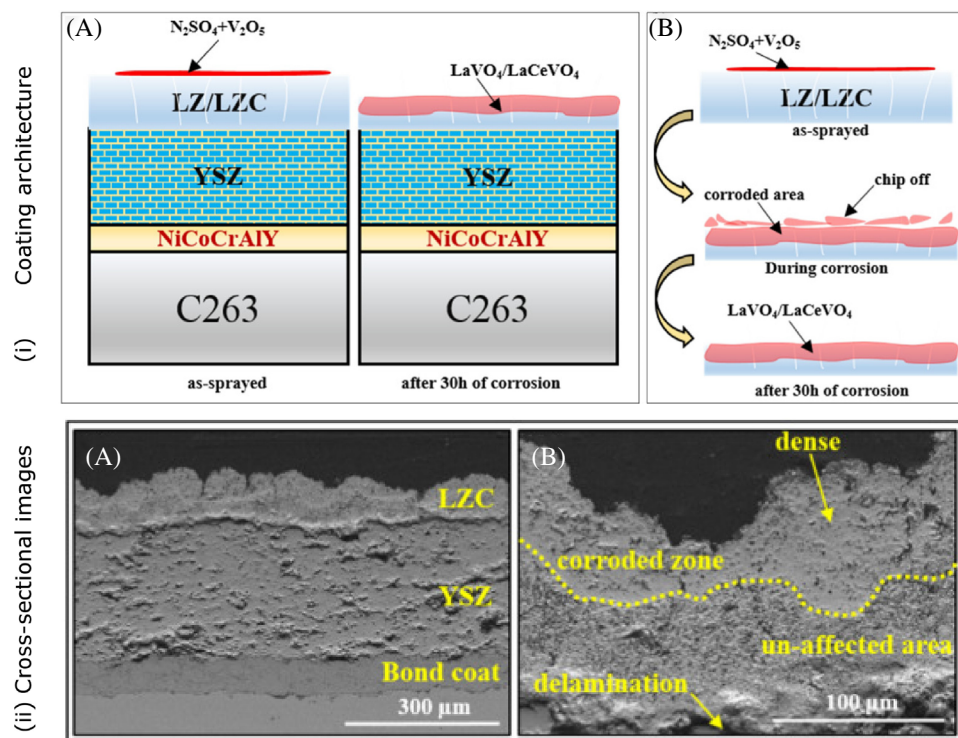


FIGURE 15 (i) (A, B) Multi-layered coating architecture of thermal barrier coatings (TBCs), and (ii) (A, B) images of double-layered LZC SPPS TBC after 30 h of corrosion at high-temperature⁸⁴ (Source: reproduced with permission).

change, inducing stress and affecting mechanical properties) of ZrO_2 . LZ coatings formed $LaVO_4$ as the primary corrosive product along with ZrO_2 and LZC coatings formed $(LaCe)VO_4$ as the primary corrosive product along with ZrO_2 . Even though the vertical cracks were present in the deposited layer, they were still defied against easy infiltration towards the YSZ layer. The LZ/LZC coatings showed inherent resistance against corrosion product infiltration which delayed coating degradation. Compared to significant degradation in conventional YSZ layer, SPPS LZ layer, the SPPS LZC layer showed better resistance despite vertical cracks. The underlying YSZ layer (in both double-layered LZ/LZC + YSZ architectures) remained unaffected by the molten salts after 30 h testing. Analysis showed that both LZ and LZC coatings acted as the sacrificial as well as molten salt corrosion resisting layer. It was concluded that the double-layered coatings could potentially improve corrosion resistance performance over the standalone YSZ layer.

For the application related to double ceramic layer thermal barrier coating, Zhang et al.⁸⁵ developed air plasma sprayed $LaPO_4$ /YSZ coatings onto Ni-based superalloy substrate with NiCoCrAlY as the bond coat and investigated hot corrosion behavior in V_2O_5 molten salt at 700, 800, 900 and 1000°C for 4 h. While the main corrosion product observed was $La(P,V)O_4$, at a higher temperature of 1000°C for the same duration, a minor amount of $LaVO_4$ was formed alongside $La(P,V)O_4$, although $La(P,V)O_4$ remained the dominant corrosion product, revealing high resistance of $LaPO_4$ /YSZ TBC's to V_2O_5 molten salt. It was recommended that $LaPO_4$ can be a promising TBC candidate for high-temperature applications, as no apparent coating degradation was observed. Roche et al.⁸⁶ investigated air plasma sprayed bilayer thermal barriers coatings of dense ceria yttria-stabilized zirconia (D-CYSZ)/yttria-stabilized zirconia (YSZ) deposited onto Inconel 625 substrate. High temperature corrosion resistance of the bilayer system was evaluated (at 900°C) using a salt mixture of 32 wt.% Na_2SO_4 and 68 wt.% V_2O_5 . Investigation showed that d-CYSZ layer had a higher resistance to high temperature corrosion, exhibiting fewer changes into the microstructure and presence of the monoclinic phase transformation despite the presence of cracks in the coating.

As discussed previously through several examples, for improved protection against molten salt corrosion, the practice has been to develop coatings with low porosity and high lamellar cohesion. It also included mitigating cracks in coating layers by managing the residual strains and phase transformation in coatings during manufacturing, as well as developing top layers which are sacrificial, can act as diffusion barrier, can have reduced scale growth, and remains resistant to molten salts, and so on. Various examples of thermally sprayed coatings considered for other aggressive corrosion resistant (other than Cu—Cl molten salt) applications are summarized in Table 2. Figure 16 presents the reported examples of thermal spray coating materials investigated under various molten salt and temperature test conditions (as per Tables 1 and 2).

2.9 | Prospects of thermal spray coatings for thermochemical cycles

There are several factors which could contribute to the cost-effectiveness of the decision to apply thermal spray coatings to thermochemical molten salt structural parts. The factors could include materials and manufacturing costs, pre- and post-manufacturing costs, maintenance costs, performance gain costs, replacement costs, and regulatory costs. Not much is known in the proposed thermochemical cycle molten salt applications, and therefore as part of further work, there is need to have techno-economic analysis, including assessing the circularity and life cycle assessment of both coatings and structural parts.

As reviewed in the sections previously, there are multiple prime design criteria which need to be considered for structural parts and overlaid coating layers, for example (Figure 17, illustrating the surface and interface issues in multilayer structure): (a) alloys as structural materials are useful when it could provide high tensile strength at elevated temperature, microstructurally stable, weldable, have long-time aging, creep rupture, and fatigue life, is MSR salt corrosion resistance, oxidation resistant, embrittlement resistant, and radiation damage resistant, and so on, and (b) coating layers (one or more layers) are useful when it could provide a thermal barrier layer, a thermal insulating layer, and a functional layer. The thermal barrier layer could enhance mechanical bonding with the top layer, could reduce the transfer of heat, provide low thermal conductivity, and mitigate thermal expansion mismatch need at the interface. Post-processing heat treatment of thermal barrier inter-layer could influence grain size and strengthen mechanical properties. Based on operating conditions, substrate material and thermochemical environmental exposure, the thermal insulating layer could provide good adhesion properties, along with minimizing heat transfer and act as barrier between the coating and the chemicals environment. The functional layers could add value to the overall coating-substrate system by providing low porosity sacrificial top layer, could be resistant to aggressive corrosion, could have good hardness, layer stability at high temperature (with lower thermal conductivity), and resistant to tribological wear, could provide no appearance change (e.g., no

TABLE 2 Literature examples (thermally sprayed coatings for other molten salt corrosion resistant applications).

Feedstock materials	Substrate	Thermal process	Molten salt mixtures	Testing details	Coating degradation related general remarks	Reference
Iron based super hard steel alloy (SHS9172)	Ferritic stainless steel/Nimonic alloy 263/Iron based alloy (SAN25)	HVOF	NaCl, Na ₂ SO ₄ , KCl with gas synthetic air +10% H ₂ O	575°C, 625°C, tested for 168 h	With some layer detachment, the coating showed good corrosion resistance.	75
YSZ (with NiCrAlY bond coat)	Ni based super alloy	APS	V ₂ O ₅	910°C, tested for 6, 12, 18, and 30 h	Coating detached from the base material in 30 hours.	80
YSZ (with CoNiCrAlY bond coat)	Ni alloy substrate (Inconel 713LC)	APS	LiCl-Li ₂ O	650°C, tested for 24–168 h	Coating showed high corrosion resistance, less reactive and good stability, proving good protection.	69
YSZ	Stainless steel (SS) type 316 L	APS	LiCl-KCl	600°C, tested for 5, 100, 250, and 500 h	Good corrosion resistance, with small weight loss.	68
YSZ, ScYSZ	Aluminium	APS	Calcium-magnesia-alumino-silicate (CMAS)	1320°C, tested for 24 and 72 h	CMAS penetrated the coating, cracks and pores appeared.	83
Al ₂ O ₃ (with CoNiCrAlY bond coat)	Ni alloy substrate (Inconel 713LC)	APS	LiCl-Li ₂ O	650°C, tested for 24–168 h.	Coating stability decreased with immersion time, and coating thickness reduced with increase in immersion time.	69
Cr ₃ C ₂ -NiCr powder blend with 75% LA-6304 and 25% LA-7319	Ni based superalloy (supermi 75)	HVOF	Na ₂ SO ₄ -60%V ₂ O ₅	1 h heating at 900°C and 20 mins cooling at room temperature for 50 cycles	Minor spallation of coating at the edges and corners at initial cycles.	72
Cr ₃ C ₂ -25(Ni-20Cr) and Ni-20Cr	ASTM-SAE213-T91 boiler steel (carbon steel)	HVOF	Na ₂ SO ₄ -60%V ₂ O ₅	900°C, 1 h of heating in furnace followed by 20 min of at cooling	Uncoated steel showed higher weight gain due to the formation of Fe ₂ O ₃ dominated oxide scales. Cr ₃ C ₂ -25(Ni-20Cr) coating more protective than the Ni-20Cr coating.	73
NiCrBSi	Ni based superalloy (supermi 75)	HVOF	Na ₂ SO ₄ -60%V ₂ O ₅	1 h heating at 900°C and 20 mins cooling at room temperature for 50 cycles	No spalling of coating on the edges and corners.	72
Co-base alloy containing Cr, W, C, Ni, Si, Fe (Stellite-6)	Ni based superalloy (supermi 75)	HVOF	Na ₂ SO ₄ -60%V ₂ O ₅	1 h heating at 900°C and 20 mins cooling at room temperature for 50 cycles	Coating spalled and peeled from the eighth cycle.	72

(Continues)

TABLE 2 (Continued)

Feedstock materials	Substrate	Thermal process	Molten salt mixtures	Testing details	Coating degradation related general remarks	Reference
Co-base alloy containing Cr, W, C, Ni, Si, Fe (Stellite-6)	High Cr-low Ni martensitic stainless steel (Boiler steel SAE 431)	Detonation gun	Na_2SO_4 -82% $\text{Fe}_2(\text{SO}_4)_3$	900°C, total duration 50 cycles on 1 h/cycle followed by 20 mins cooling	Cracking and degradation in coatings appeared.	76
Ni-20Cr (wire form)	Ni based superalloy (supermi 75)	HOVF	Na_2SO_4 -60% V_2O_5	1 h heating at 900°C and 20 mins cooling at room temperature for 50 cycles	Negligible amount of spalling at edges and corners.	72
Ni20Cr	18% Cr and 8% Ni austenitic grade steel (stainless steel 304)	HOVF	ZnCl_2 -KCl	350, 400, 450°C, test performed in the crucible with furnace, molten salt, and SS rod as a working electrode	Molten salt penetrated the coatings layer, and corrosion current density increased gradually with the increase in temperature.	77
Co-base alloy containing Cr and Mo (Stellite-21)	High Cr-low Ni martensitic stainless steel (Boiler steel SAE 431)	Detonation gun	Na_2SO_4 -82% $\text{Fe}_2(\text{SO}_4)_3$	900°C, total duration 50 cycles on 1 hour/cycle followed by 20 mins cooling	Coating showed low stability, and cracks propagated to the centre of coating.	76
SYSZ (with NiCrAlY bond coat)	Ni based super alloy	APS	V_2O_5	910°C, tested for 6, 12, 18, and 30 h	Coating showed high degradation due to the crack formation, degradation observed after 30 hours, and microcracks formation in coating accelerated the corrosion rate.	80
CYSZ (with NiCrAlY bond coat)	Nickel based super alloy (Inconel 738)	APS	45 wt% Na_2SO_4 + 55 wt% V_2O_5	1000°C, tested for 6–300 h	Minor portion of the coating came apart from the corner due to thermal stress, and it withstood the hot corrosion environment for 300 h.	82
Ni50Cr		HVOF	40 wt% K_2SO_4 , 40 wt% Na_2SO_4 , 10 wt%KCl and 10 wt%NaCl	550°C, tested for 100 h	Chlorine penetrated all over the coating and it showed degradation, and chromium was selectively attacked by chloride.	70

(Continues)

TABLE 2 (Continued)

Feedstock materials	Substrate	Thermal process	Molten salt mixtures	Testing details	Coating degradation related general remarks	Reference
Ni50Cr	-	HVOF	40 wt% K ₂ SO ₄ , 40 wt%Na ₂ SO ₄ , 10 wt%KCl and 10 wt%NaCl	550°C, tested for 100 h	Chlorine penetrated all over the coating and potassium at some places, and coating showed excellent corrosion resistance, with some cracks and partially disintegration observed.	70
Ni57Cr	-	HVOF	40 wt% K ₂ SO ₄ , 40 wt%Na ₂ SO ₄ , 10 wt%KCl and 10 wt%NaCl	550°C, tested for 100 h	Coating could not protect the substrate from the corrosion.	70
Ni21Cr9Mo	-	HVOF	40 wt% K ₂ SO ₄ , 40 wt%Na ₂ SO ₄ , 10 wt%KCl and 10 wt%NaCl	550°C, tested for 100 h	Plenty of chlorine, some potassium and sodium were detected at the coating substrate interface, substrate was massively attacked, with severe oxidation attack on the splat boundaries.	70
Intermetallic (Fe ₃ Al)	-	HVOF	40 wt% K ₂ SO ₄ , 40 wt%Na ₂ SO ₄ , 10 wt%KCl and 10 wt%NaCl	550°C, tested for 100 h	Chlorine detected at the splat boundaries, coating was severely oxidized and corroded, along with degradation of all coating areas and substrate also observed.	70
80Ni20Cr	Steel: 9% chrome, 1% molybdenum, with deliberate addition of vanadium and niobium (T91)	HVOF	Na ₂ SO ₄ -60%V ₂ O ₅	750°C, under cyclic temperatures 50 cycles, 1 h heating at 750°C and 20 min cooling at room temperature	Showed low level of weight gain, with no change in the coating surface.	71
75Cr ₃ C ₂ -25(Ni-20Cr)	Steel: 9% chrome, 1% molybdenum, with deliberate addition of vanadium and niobium (T91)	HVOF	Na ₂ SO ₄ -60%V ₂ O ₅	750°C, under cyclic temperatures 50 cycles, 1 h heating at 750°C and 20 min cooling at room temperature	Little changes in the coating surface.	71

(Continues)

TABLE 2 (Continued)

Feedstock materials	Substrate	Thermal process	Molten salt mixtures	Testing details	Coating degradation related general remarks	Reference
Ni-Cr	Ferritic stainless steel-based alloy (SAN25)	HVOF	NaCl, Na ₂ SO ₄ , KCl with gas synthetic air +10% H ₂ O	575°C, 625°C, tested for 168 h	Coating showed better corrosion resistance.	75
Diamalloy 4006	Ferritic stainless steel	HVOF	NaCl, Na ₂ SO ₄ , KCl with gas synthetic air +10% H ₂ O	575°C, 625°C, tested for 168 h	The deposition contained mainly iron, chromium, oxygen and small amount of chorine, potassium, and sulfur. Coating showed significant corrosion and corrosive product deposits.	75
Fe-25Cr-15W-1.2Nb-6Mo or SHS9172	Ferritic stainless steel	HVOF	NaCl, Na ₂ SO ₄ , KCl with gas synthetic air +10% H ₂ O	575°C, 625°C, tested for 168 h	Corrosive product deposits, with slight detachment, and oxide layer contained iron, chromium, and sodium.	75
Ni-based superalloys (IN625)	Ferritic stainless steel/Nimonic alloy 263/iron based alloy (SAN25)	HVOF	NaCl, Na ₂ SO ₄ , KCl with gas synthetic air +10% H ₂ O	575°C, 625°C, tested for 168 h	Coating showed better corrosion resistance, with localized coating layer detachment.	75
NiCrBSiFe	Steel: 9% chrome, 1% molybdenum (P91)	HVOF	K ₂ SO ₄ -KCl	525, 625, 725°C, tested for 168 h	Very little corrosion products deposited on coating, with little or no significant effect on the substrate.	74
Ni-based superalloys (Ni alloy 718)	Steel: 9% chrome, 1% molybdenum (P91)	HVOF	K ₂ SO ₄ -KCl	525, 625, 725°C, tested for 168 h	Coating degradation and delamination increased with the increase in temperature, and presence of chlorine at the coating-substrate observed.	74
Ni-based superalloys (IN625)	Steel: 9% chrome, 1% molybdenum (P91)	HVOF	K ₂ SO ₄ -KCl	525, 625, 725°C, tested for 168 h	Coating degradation and delamination observed.	74

(Continues)

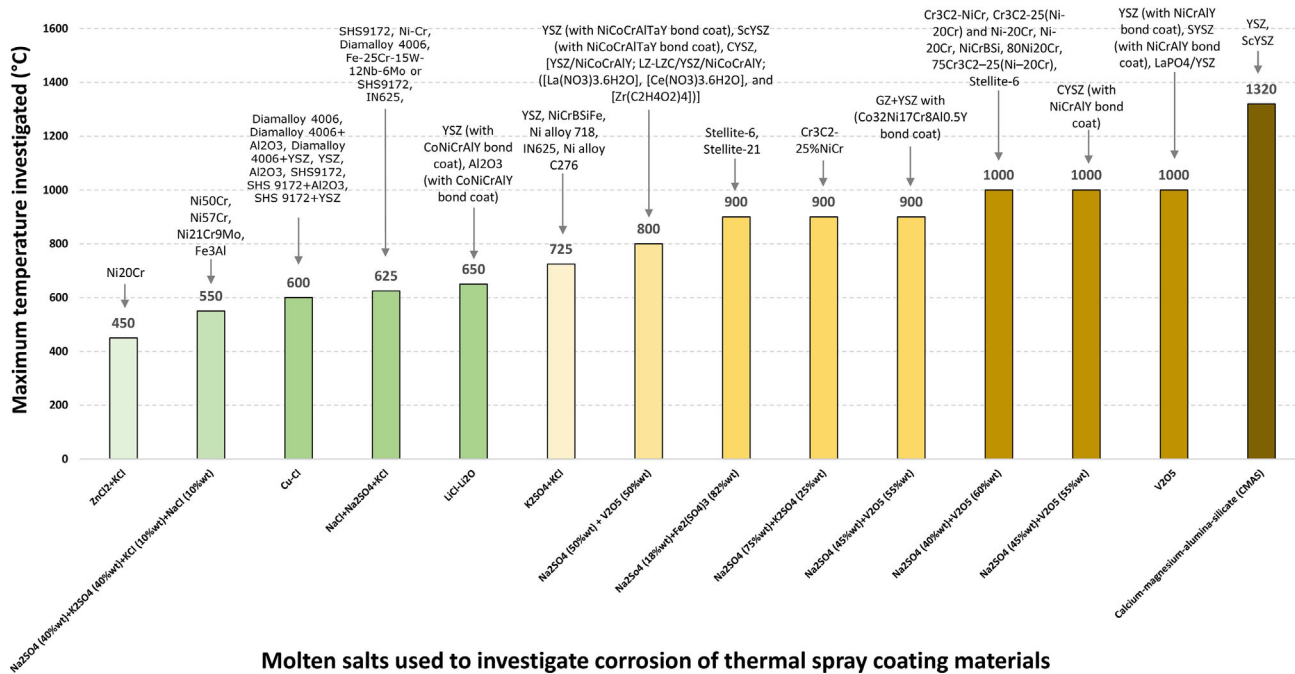
TABLE 2 (Continued)

Feedstock materials	Substrate	Thermal process	Molten salt mixtures	Testing details	Coating degradation related general remarks	Reference
Ni-Mo-Cr alloy with a small amount of W (Ni alloy C276)	Steel: 9% chrome, 1% molybdenum (P91)	HVOF	K ₂ SO ₄ -KCl	525, 625, 725°C, tested for 168 h	High level of corrosion and oxide formation observed in coating.	74
YSZ, Ni-25Co-20Cr-8Al-4Ta-0.6 (wt.%) (bond coat)	Ni-based superalloy (IC 10)	APS	Na ₂ SO ₄ + V ₂ O ₅	1000°C, sample placed in the electrical furnace	High temperature resulted to corrosion products deposition, and large salt crystals formed on the coating.	78
ScYSZ, (with NiCoCrAlTaY bond coat)	Nickel based superalloy	APS	Na ₂ SO ₄ + V ₂ O ₅	1000°C, sample placed in the electrical furnace	No corrosion product on the coating, no effect of the corrosive degradation, and the coating showed superior chemical stability and phase stability.	78
Cr ₃ C ₂ -25%NiCr	Ni based superalloy (Superni 75)	Detonation gun	75 wt% Na ₂ SO ₄ + 25 wt% K ₂ SO ₄	900°C, tested for 100 cycles	Nickel observed at the interface where chromium was depleted.	79
Cr ₃ C ₂ -25%NiCr	Ni based superalloy (Superni 718)	Detonation gun	75 wt% Na ₂ SO ₄ + 25 wt% K ₂ SO ₄	900°C, tested for 100 cycles	Chromium and nickel observed on top of the coating, and nickel observed at the interface where chromium was depleted.	79
Cr ₃ C ₂ -25%NiCr	Ni based superalloy (Superfer 800H)	Detonation gun	75 wt% Na ₂ SO ₄ + 25 wt% K ₂ SO ₄	900°C, tested for 100 cycles	Chromium and nickel observed on top of the coating, and nickel observed at the interface where chromium was depleted.	79
YSZ/NiCoCrAlY; LZ-LZC/YSZ/NiCoCrAlY; ([La(NO ₃) ₃ ·6H ₂ O], [Ce(NO ₃) ₃ ·6H ₂ O], and [Zr(C ₂ H ₄ O ₂) ₄])	Aluminium-titanium age hardened nickel base superalloy (C263)	APS, SPPS	50wt.%Na ₂ SO ₄ + 50wt.%V ₂ O ₅	800°C, tested for 30 h	Corrosion products deposition increased with the time. SPPS LZ and LZC coatings acted as the sacrificial as well as resisting layer against molten salt corrosion. Double-layered coatings improved performance over the standalone YSZ system. In both double-layered LZ/LZC + YSZ architectures, the underlying YSZ remained unaffected by the molten corrosive salts after 30 hours.	84

(Continues)

TABLE 2 (Continued)

Feedstock materials	Substrate	Thermal process	Molten salt mixtures	Testing details	Coating degradation related general remarks	Reference
LaPO ₄ /YSZ	Ni-based superalloy	APS	V ₂ O ₅	700–1000°C, tested for 4 h	Temperature did not change the phase and smoothness of coating. LaPO ₄ /YSZ TBCs showed high resistance to V ₂ O ₅ molten salt. LaPO ₄ can be a promising TBC candidate for high-temperature applications.	85
CYSZ, YSZ	Nickel-chromium alloy (IN625)	APS	Na ₂ SO ₄ + V ₂ O ₅	900°C, tested for 10 h	Long temperature cycles reduced thickness of coatings and delamination was observed. YSZ showed high density of splat cracks. CYSZ showed vertical cracks and cracks intensity decreased with increase in thickness. d-CYSZ layer resulted in an efficient barrier to the molten salt attack since the bilayer systems presented less morphological and microstructural degradation than the YSZ system. Inclusion of LP-YSZ layer improved thermal shock resistance by increasing stiffness, providing resistance against external stresses, thermal expansion mismatch, and irregular growth of thermally grown oxide (TGO).	86
GZ + YSZ with (Co32Ni17Cr8Al0.5Y bond coat)	Ni22Cr1.5Co 0.5W9Mo18Fe1Si (Hastelloy X)	SPS	55 wt.% V ₂ O ₅ and 45 wt.% Na ₂ SO ₄	900°C, tested for 8 h	Good interface adherence between coatings. No coating spallation observed. The columnar gaps in the double and triple layer SPS coating effectively facilitated molten salt infiltration, and the inert nature of the molten salts with the topcoat material caused overflow and damage from the coating's edge to its centre. The sealing layer in the triple-layer system proved ineffective, reducing the number of infiltration channels for molten salts, leading to higher overflow and more damage.	81



Molten salts used to investigate corrosion of thermal spray coating materials

FIGURE 16 Mapping the reported examples of thermal spray coating materials investigated under various molten salt and temperature test conditions (data extracted from Tables 1 and 2) (Source: authors original image).

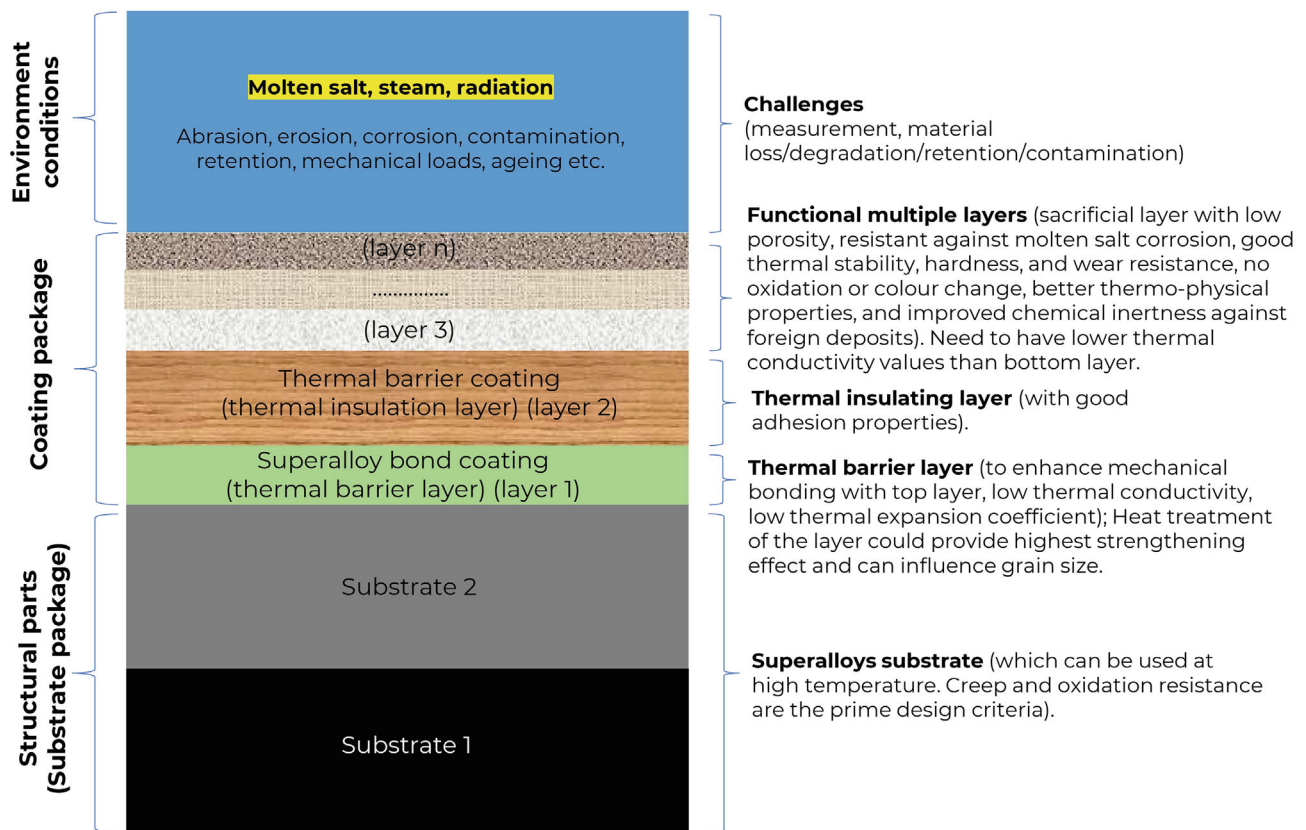


FIGURE 17 Illustrating the surface and interface related issues in multilayer structure (presenting conceptual multi-layered coating-substrate system to mitigate various molten salt environment conditions) (Source: authors original image).

oxidation) to the top layer, could have better overall thermo-physical properties, and provide improved chemical inertness against foreign deposits (liquid/solid).

2.10 | Laboratory-based reactor design and immersion testing requirement

As expected for a molten salt reactor (MSR), the primary nuclear reactor coolant and/or the fuel is a molten salt mixture at high temperature. Therefore, testing and qualification of materials (coatings and substrates) require special equipment and procedures, as such testing are typically carried for an extended period to study the effect of molten salt.

In such work, the coatings are typically exposed to the conditions of molten salt reactor for extended period (e.g., 100 h or more) in the absence of oxygen. The testing reactor design requires some consideration, so that during testing the absence of oxygen in the system can be ensured. It also requires designing a new geometry of sample so that coating integrity on the sharp edge of the sample could be mitigated, and where the immersion tests of samples can be conducted for extended period. The testing should help assess the results of various materials after immersion tests and other characterization and monitoring studies.

Majority of the analysis of coatings have been carried out through immersion test. This includes design of an immersion test vessel typically as per ASTM G31-21 (Standard Guide for Laboratory Immersion Corrosion Testing of Metals), where mainly mass loss tests could be carried. In such immersion tests, the test conditions, for example test chemical composition, temperature, gas sparging, liquid motion, volume, method of supporting (holding) test samples, and duration of test could be varied and investigated.⁸⁷ However, such standard test set-up does not allow measurement of cracking, coating delamination or other effects, such as solution flow.

Siantar³⁶ and Naterer et al.²⁹ have described the laboratory-based immersion test and procedures to handle such tests in much detail with the design and actual test apparatus shown in Figure 18A,B. The design of such reactor and immersion test set-up requires special consideration. Overall, all we need is a safe testing environment during molten salt immersion testing. These include fume hood enclosure (to allow molten chemical and gaseous waste to escape in safe direction), high temperature protection due to filling the crucible with molten salt, followed by post-immersion cleaning of the equipment and sample recovery for further analysis. The immersion vessel structural materials which house molten salt should be chemically inert and should not react at high operating temperatures, should be sealed, and leak-free. They proposed fused quartz as vessel structural material which is a better candidate material for high temperature applications (with softening point at 1730°C, higher than the immersion test operating temperature at 500°C), which does not expand much during extended heating, as well as it is an inert material. Other part of the test set-up could be made using other traditional materials (such as stainless steel, borosilicate glass, Teflon, rubber, polyethylene, etc.) as those are far from the heat source and molten salt. For measurement purpose, the vessel should have inlets and outlets for thermocouple and connecting pipes, as well as pressure relief device for inert gas flow. The heating system with appropriate safety

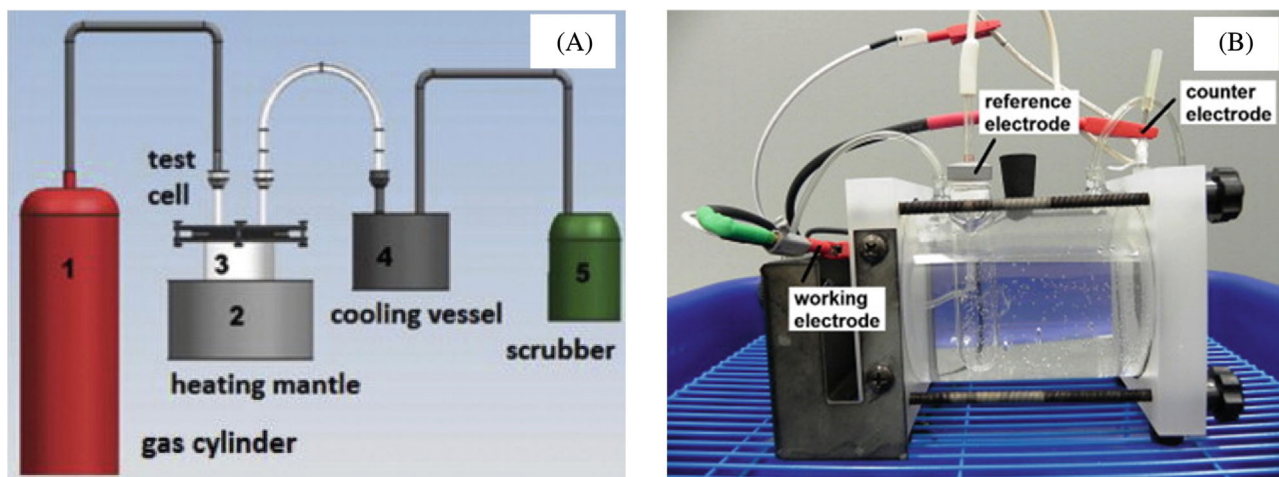


FIGURE 18 Immersion test model set up: (A) same test set-up presented in simplified way by Naterer et al.,²⁹ and (B) electrochemical cell for corrosion testing⁸⁸ (Source: reproduced with permission).

should heat the outer side of the immersion vessel. To mitigate air pollution and ensuring that the processes comply with emissions standards and regulations, the scrubber is also needed to offset the gaseous waste and redundant chemicals transported by the purge gas.

Apart from weight loss method, electrochemical methods could be used to quantify corrosion rates in mm/year. Electrochemical corrosion testing includes 2- or 3-electrode (i.e., counter, reference, and working) electrochemical impedance spectroscopy (EIS) equipment and other accessories. The working electrode is typically the materials to be tested (coatings and substrates), while the counter electrode is typically platinum wire and reference electrode could be any, for example, Ag/AgCl. Figure 18B shows the corrosion test cell at room temperature (not high temperatures) corrosion measurement.⁸⁸

Similar to methodology presented previously, Azhar⁵⁸ have also used laboratory-based immersion test and procedures to test various specimens, as shown in Figure 19A–E. The experimental setup included a temperature controller,

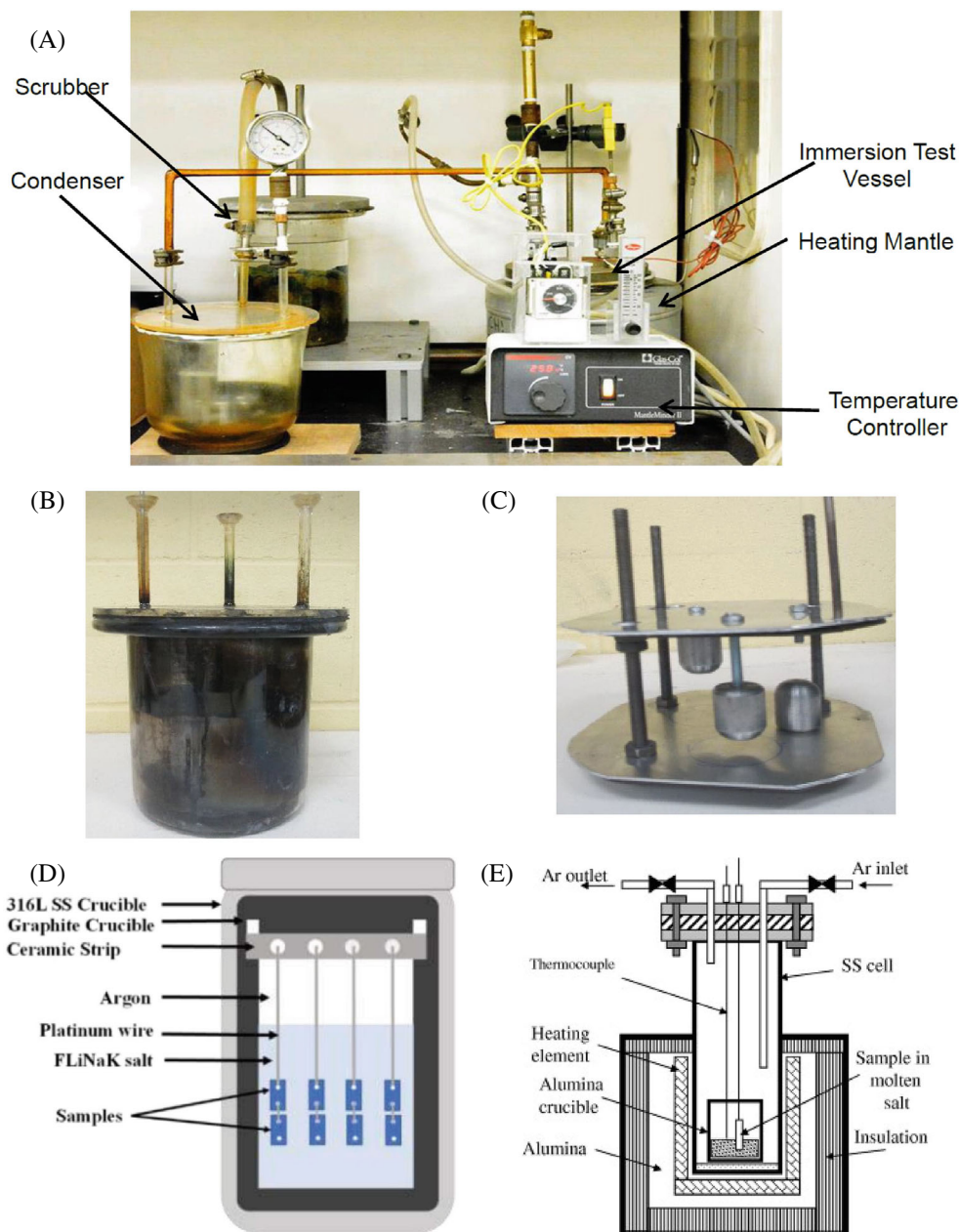


FIGURE 19 (A) High temperature molten salt corrosion testing lab set-up⁵⁸; *Source*: permission obtained ©M.S. Azhar, all rights reserved, (B) immersion test vessel⁵⁸; *Source*: permission obtained ©M.S. Azhar, all rights reserved, (C) sample handling and lifting mechanism⁵⁸; *Source*: permission obtained ©M.S. Azhar, all rights reserved), (D) alternative design of corrosion test set-up³⁸ (*Source*: reproduced with permission), and (E) specifically designed test cell⁶⁸ (*Source*: reproduced with permission).

condenser, scrubber, and immersion test vessel (made of quartz glass, for testing up to 1050°C) in the fume hood which ventilates toxic and hazardous gases. It was suggested that glass is the only material that could be used for this purpose as other material was not able to withstand such high temperatures with Cu—Cl environment. Considering the sample holding and handling during the immersion tests, Azhar⁵⁸ simplified this with the use of two stainless steel plates arranged in a parallel way with screws and rods (Figure 19C).

For structural samples (non-coated metallic substrates), Li et al.³⁸ proposed a method to test multiple samples in a molten FLiNaK bath (LiF-NaF-KF: 46.5–11.5–42 mol%), where separate samples were hung up and experiments were carried in an Ar-filled glove box to avoid the influence of excess water and oxygen (Figure 19D). In this method, the crucible (made of graphite) was filled with FLiNaK salts and was placed into a 316 stainless steel crucible (sealed by welding as well as heated in a furnace at 650°C for 100 h). As shown in Figure 19E, Shankar et al.⁶⁸ developed corrosion test cell for testing coated samples in molten LiCl–KCl salt. In custom built test cell, the stainless-steel cell along with the test sample could be taken into an Ar-atmosphere glove box. The salt could then be loaded in the Al₂O₃ crucible and could be placed in the stainless-steel cell, along with test sample and thermocouple for temperature measurement, following which the cell could then be sealed inside the glove box.

3 | OPPORTUNITIES AND CHALLENGES

3.1 | Design and modeling work

While there is an opportunity to advance the material, manufacturing, characterization, testing, and qualification methods for thermochemical cycle electrolysis, it also requires developing theory and modeling. As part of the theory and modeling work, the research should be covering all stages of investigation of materials design (from molecular to macroscale) to product development, including validation, characterization, and life cycle assessment (LCA). The approach should help translate industry needs (in relation to electrolysis-based hydrogen production) into innovation challenges and provide solutions to multi-component parts or structures. To achieve the above outcomes, with the combination of theory and modeling approaches, focusing on user cases, the research should have a clear demonstration of modeling (e.g., Figure 20, illustration based on schematic shown in Figures 1 and 5) and system integration, including various development stages of materials and final products.

To establish a theoretical and modeling database for predicting structural design, assembly, and operational challenges in the thermochemical module for hydrogen production application, various methods, and approaches (e.g., Monte Carlo, finite element, and computational fluid dynamics) could be applied. The modeling could establish a design of

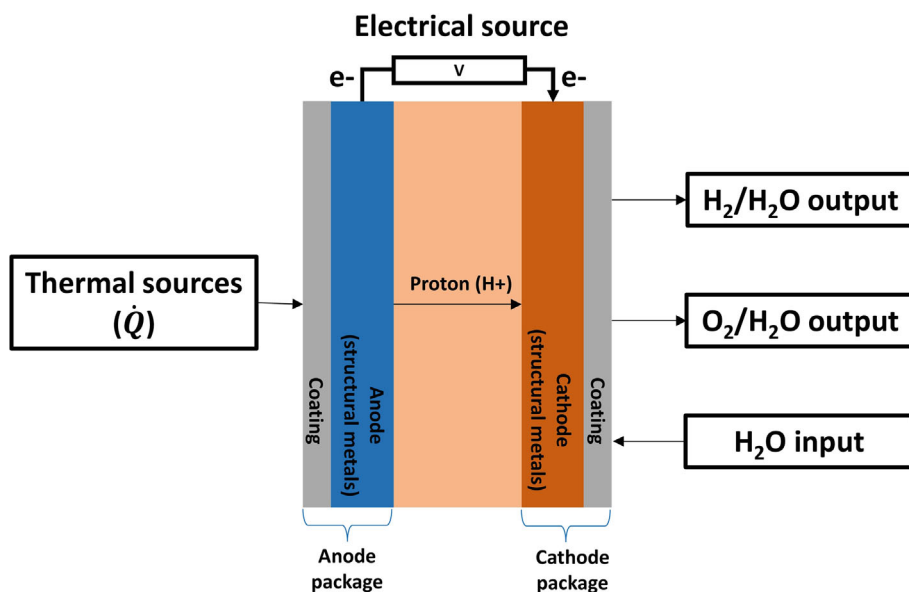


FIGURE 20 Illustrating the basic input and output in a nuclear thermochemical cycle electrolysis cell (Source: authors original image).

the coating-substrate system, and operational challenges in the electrolyser unit hydrogen production. For appropriate structural behavior, the coating-substrate system must be thermo-mechanically and thermo-chemically well-controlled and able to be reproduced. Using theoretical and modeling methods, which can offer further detailed views of the application process and can show the effect of different operating conditions (e.g., thermo-mechanical loads and unloading conditions, incidental loads, durability, transient behavior, current distribution, single/multiphase flow, etc). Any design optimisation usually requires expensive trial and error practices and procedures, therefore modeling and simulation of the coating-substrate system operation and processes involved are very useful. Modeling will bring together the links between the design-structure-property relationship which will acknowledge the effect of operational parameters, electrode design and materials chosen.

Benchmarking of coating-substrate system in thermochemical cycle structural parts could be an important criterion for various reasons. The coating-substrate system needs to be designed for high temperature thermochemical deployment applications, and benchmarking needs to be done specifically for sector requirement (e.g., nuclear reactor heat transfer). Issues such as operating conditions in a radiological and chemical environment, restricted access, reduced cost, enhanced structural integrity and aligned to regulatory standards, enhanced efficiency, materials selection which can operate at high temperature, accounting for corrosion rates, and design needs to be considered. The benchmarking work should focus on process-property relationship models and material laws definition to apply in structural analysis and design optimisation within the allowable limits for the cell design and manufacturing processes.

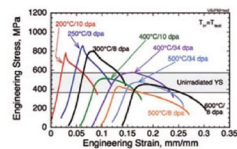
There is need to develop a base for design, manufacture, and test tasks to define the reactor specifications using literature and industrial input considering current regulatory, knowledge and technology gaps in such field. The modeling study should focus on design integrity, structural and thermo-mechanical loading and unloading conditions (internal, external, and deployment), incidental loads (impact and shock) and durability (cyclic loadings, vibration, and material degradation) to enable the critical application capability. The analysis should be able to help understand the design and dimensioning of the components. Implementation of the thermal expansion into the structural model could allow evaluating the stress distribution in the reactor during a variation of operating conditions. Analysis and establishing how fluid and by-products diffuse into the materials, investigating the effects of porosity, tortuosity, and thickness of the coating materials is also critical. Finally, the study of heat generation and transfer could also help in defining optimized thermal management.

3.2 | Management of radiation-induced damage and potential contamination of materials

Nuclear radiation particles (alpha, beta, gamma, and neutron) generated due to fission reaction in nuclear reactors have various penetration range into the materials, which could contaminate and damage the structural materials. Particles (e.g., protons, alpha-particles/helium nuclei, beta-particle/fast neutrons or positrons, and fission fragments), could transfer enough energy through elastic or inelastic collisions to remove nuclei from their lattice positions, and therefore, such addition of vacancies and interstitial atoms could cause changes in material properties. Radiation-induced crystallographic defects due to vacancies (or knock-ons), interstitials, ionization, thermal and displacement spikes, impurity atoms, and radiation-induced creep could all have effect of greatest interest on materials.⁸⁹ As shown in Figure 21, nuclear radiation damage to structural materials poses some threats to the operation of structural parts.⁹⁰ In practical terms, the damage could be in the form of radiation hardening and embrittlement (reduced elongation and fracture toughness), phase instabilities, irradiation creep, void swelling, corrosion, stress corrosion cracking, and more.^{90,91}

It is important to be clear that the radioactive contamination of the structural parts (materials) is not well understood while developing complex multi-layer structures like nuclear thermochemical reactors for hydrogen production through electrolysis. The structural parts (e.g., pipelines and vessels) in the vicinity of nuclear fuel (fissile product) mixed with molten salt could be contaminated due to the presence of ionizing radiation due to radioactive decay of the contaminants. Also, the radiation-induced damage of structural materials needs to be understood for material selection, as this could help in evaluating the structural materials in-reactor degradation behaviors.⁹⁰⁻⁹⁴ Satisfying standard materials design criteria based on various mechanical properties (e.g., tensile, creep, and fatigue) is critical for structural parts for nuclear energy systems. Overall, the selected materials should provide adequate resistance to radiation damage and should show chemical compatibility.^{90,91}

In traditional design, there are structural parts in nuclear power reactors which are tubular or thin plate in shape. These include zirconium (Zr)-based nuclear fuel cladding tubes, thin-plated grids in light water reactors, and oxide



- **Radiation hardening and embrittlement** ($<0.4 T_M, >0.1 \text{ dpa}$)
- **Phase instabilities from radiation-induced precipitation** ($0.3\text{--}0.6 T_M, >10 \text{ dpa}$)
- **Irradiation creep** ($<0.45 T_M, >10 \text{ dpa}$)
- **Volumetric swelling from void formation** ($0.3\text{--}0.6 T_M, >10 \text{ dpa}$)
- **High temperature He embrittlement** ($>0.5 T_M, >10 \text{ dpa}$)

FIGURE 21 Nuclear radiation damage threats to structural materials performance⁹⁰ (Source: reproduced with permission).

dispersion-strengthened (ODS) steel claddings in fast breeder reactors.⁹³ Considering the manufacturing of such parts, they are fabricated which consist of plastic deformation process (e.g., cold/hot rolling, extrusion, and/or pilgering), leading to formation of inhomogeneous microstructures. Such deformation could lead to anisotropic mechanical properties as well as in-reactor degradation over time.

There are established protocols to manage the sources of contamination, its containment, control, and monitoring of contamination, decontamination, assessment of contamination hazards, nuclear waste handling and disposal, etc. However, for nuclear thermochemical electrolysis (which is a multi-layer structure made of different materials), the effect of radioactive contamination and degradation of structural parts is not well understood or not explored much. This means more research is needed to determine structural contamination, its degradation and to put in place necessary measures for a sustainable electrolysis process. One of the important actions could be the application of radiation-shielding materials (for example, traditional lead (Pb) or lead composite shielding) which could help attenuate the radiation level into the material. Noteworthy, Pb is soft, malleable and corrosion resistant material. Alternatively, the application of Pb-free shielding materials which could provide similar protection levels, which could be tin, antimony, tungsten, or bismuth, however, further investigation is needed.

For nuclear energy system based thermochemical cycle electrolysis to reach their full potential, high performing structural materials are needed that incorporate improved mechanical strength, adequate ductility, and fracture toughness, along with good radiation resistance, and high temperature corrosion resistance. Multiphysics computational modeling approach, and experimental validation will be needed to demonstrate the stability of new structural alloys and coating materials under prolonged exposure to high temperature, mechanical stress, and nuclear irradiation.

4 | MISCELLANEOUS OPPORTUNITIES

4.1 | Alternative manufacturing for aggressive corrosive environments

Manufacturing for aggressive and harsh corrosive environments (such as high temperature and pressure, corrosive and high radiation levels, and potentially other demanding factors) involves the production of structural and coating parts that can sustain and reliably perform under harsh and challenging conditions. Due to the lack of structural materials which can withstand the high temperature corrosive environment, commercialisation of MSRs technology is significantly

hindered.³⁸ Development of new alloys, possibly combined with advanced deposition or coating methods, with enhanced mechanical properties, resistance to corrosion in molten salts and radiation damage should be considered.

Manufacturing techniques continue to evolve rapidly, and new approaches have gained traction to manufacture alloys and coatings which could assist in enhancing the properties. Utilization of alternative manufacturing techniques can be considered such as additive manufacturing (AM), laser processing, powder metallurgy, and potentially application of nanotechnology to produce structural and coated components with better performance. Additive manufacturing has allowed the use of high-temperature resistant materials, such as Ni-based superalloys and refractory metals, which are crucial for components operating in extreme heat environments.⁹⁵ It can also produce intricate geometries that are challenging to achieve using traditional manufacturing methods, however further research is needed to find if additive manufactured components could improve performance and efficiency in thermochemical extreme environments. This becomes more important as additive manufacturing could allow for rapid prototyping and customisation for complex shapes, rapid repair, and maintenance, potentially reducing downtime, and creation of radiation tolerant structures.

Laser cladding, also known as laser metal deposition, is a new type of surface engineering or coating technology. During this process, the cladding powder melts and solidify on the substrate under the irradiation of laser beam (high power laser as a heat source). Coating layers deposited by laser cladding for molten salt reactors serve multiple purpose, ranging from hard, self-lubricating, high temperature oxidation resistant, to wear and corrosion-resistant layers. Laser clad layer forms a metallurgical bond with the substrate (good adhesion with the substrate), heat-affected zone are small, and forms a fine microstructure due to large temperature gradient. Laser clad coated layers have been developed from a single crystal alloy, amorphous alloys, multiple-alloy, multiple-ceramics, high entropy alloys (HEAs).^{96,97}

Powder metallurgy technique has allowed the use of refractory metals and alloys that can withstand extreme heat conditions, can enabling the production of components with complex shapes, can help achieve uniform microstructures, can incorporate various materials and additives leading to the creation of composite structure, and can have reduced material waste. As an example, Li et al.³⁸ used powder metallurgy method and prepared 1 wt.% Y_2O_3 dispersion-strengthened NiMo-based alloys as structural materials and demonstrated its higher ultimate tensile strengths and yield strengths than the Ni-based alloy (Hastelloy N).

4.2 | Reliability assessment opportunity

Reliability analysis for a thermochemical electrolysis system could be based on system level physical modeling and experimental results for degradation. As seen through various research, there could be various reasons that may cause degradation or failure of nuclear thermochemical cycle structural parts (such as anode package, cathode package, membrane). Monitoring and analyzing such systems are important, like other similar structures or multi-stack systems (e.g., solid oxide fuel cell or SOFC,⁹⁸ or other unrelated fields). While degradation of materials and structural parts can lead to failure, but other factors could also lead to failure, which could be excessive current densities, cyclic power supply (i.e., start-up and shut down cycles), and associated failure probabilities. Additional factors could also lead to failure such as variation between steady and transient state operations, sudden mechanical shock to structural parts (due environmental factors), including any human handling error.

As discussed previously, the structural parts of electrolysers are made up of layers of metals and coatings (alloys, ceramic, and cermets), the flaws could be in both substrate and coatings, and the failure probability could be more in the anode part due to its direct interaction with molten salt. For long-term stability of the thermochemical cycle structural parts and coating materials, an adequate match and compatibility in terms of thermo-mechanical and thermo-chemical properties is important. One of the important physical quantities to monitor during operation of a combined thermochemical cycle electrolysis system is heat input at the anode side and heat distribution to rest of the structure (coating and substrate system). High temperature corrosive environment has a strong effect on several structural degradation mechanisms, also on performance and durability on system level. Stack system failure could lead to changes in voltage and current density due to an increased power density per stack, as typically known for solid oxide fuel cell system.⁹⁸ As part of future development, development of models representing the relationship between electrical voltage and current density, and failure probability function using temperature as primary variable could be necessary.^{98,99} Also, the development of correlation between stresses and failure probability should be considered, which could establish the link between current density and failure probability.^{98,100}

As proposed by Colombo and Kharton,⁹⁸ a methodology for SOFC, development or implementation of similar or modified methodology to conduct a system reliability analysis for nuclear thermochemical electrolyser could be considered.

This could include system design (or flow diagram of the process), weakest element(s) identification in one unit (a system which could have multiple units), performance characteristics construction (experimental data and Multiphysics model), stack level virtual aging due to degradation, system level identification of potential failure phenomena, unit level construction of relationship between performance metrics and failure probability, combined calculation of failure probability of the system, development of technological case studies, and then translation of failure behavior into financial metrics which includes capital, operation expenditure and downtime. As there is limited literature available in thermochemical cycle electrolyser, proposed reliability analysis and engineering design principles for SOFC system may act as an opening for related system analyses, as recommended by Colombo and Kharton.⁹⁸

4.3 | Life cycle assessment opportunity

Ambition to have a cost saving strategy and sustainable sourcing of feedstock materials (or development of new materials) is important part of nuclear thermochemical electrolysis, and this should be addressed through further research. For a sustainable energy supply through electrolysis soon, the technologies should be environmentally burden free. Considering the entire life cycle of the process and value chains, a life cycle assessment (LCA) is necessary to identify such impacts.^{101–103} LCA is an established and internationally accepted method that is defined in the ISO standard (e.g., ISO14040-14044). It refers to the activities during the product's lifetime from its manufacturing, through use and maintenance to its raw material circulation required to re-manufacture the product (cradle-to-cradle).¹⁰⁴

As reviewed by Bhandari et al.,¹⁰¹ electrolysers have traditionally been analyzed as a unitary system, and therefore, details on the contribution from individual parts could not be understood from previous work. Considering different materials and service lifetimes of parts as well as the use of environmentally friendly materials, a more disaggregated evaluation could be interesting because it can distinguish between the different nuclear thermochemical cycle electrolyser types, and not just their supply of energy. LCA focused on an electrolyser unit (thermochemical cycle electrolyser in the current context) should be carried out to understand the contribution of individual parts. By including other impact categories beyond the global warming potential (GWP), the research should also broaden the scope of the LCA studies. Nuclear thermochemical cycle electrolyser focused life cycle analysis would be an important investigation, for example, when toxic impacts on coating and structural materials caused by nuclear contamination are analyzed.

4.4 | Techno-economic analysis opportunity

Thermal spray coating is an integral part of various industrial sectors (e.g., aviation, transportation, power generation, chemical and biomedical industry), with a global worth of around USD 11.37 billion in 2024 to USD 13.98 billion by 2029, growing at a CAGR of 4.22% (during forecast period 2024–2029).¹⁰⁵ Techno-economic analysis on the application of thermal spray coatings for thermochemical cycle structural parts followed by the development of an electrolyser system could help to assess its technical feasibility and economic viability. While such analysis is not sufficiently available, it could be important to understand the potential economic benefits, risks, and barriers associated in adopting thermochemical cycle electrolysis.^{65,66,106} In such analysis, a range of considerations are needed for thermochemical cycle electrolysis, such as (a) process description (chemical reactions, materials requirement, sources of energy and description about other components or products), (b) to set-up the facility, analysis of capital and operational costs are needed, (c) overall energy efficiency analysis as well as energy consumption analysis are needed, (d) market analysis for revenue generation, (e) sensitivity analysis to assess the overall economic viability, (f) technical uncertainty analysis of immature technology, (g) environmental risk assessment and impact, and (h) financial and regulatory analysis. These analyses will help end users, developers and stakeholders make informed decisions and guide future opportunities.

4.5 | Standards and regulation opportunity

Currently, there are no specific standards dedicated solely to thermochemical cycle electrolysis. However, relevant existing standards from different domains could be applied which covers safety, materials, environmental impact, and other aspects related to the technology and its operation. Within such opportunities, considerations about the coating and structural materials are needed, such as (a) safety standards, (b) environmental standards, (b) chemical standards, (c) materials

standards, (d) energy efficiency and sustainability standards, and (e) quality and reproducibility standards. Since different countries could have specific regulations or guidelines to address aspects of thermochemical cycle electrolysis, it could be essential to engage stakeholders, organizations, and regulatory bodies to identify and adhere to the most applicable standards and guidelines. At best in short term, awareness about the latest developments in the field could also help ensure compliance with the best practices.

Similarly, regulations could vary by country, and it may cover various aspects, including safety, environmental impact, operational procedures, and more. Some areas of regulation for thermochemical cycle electrolysis could include: (a) safety regulations to ensure the safe handling of chemicals, hazardous materials, equipment, and operating procedures, processes and safety protocols for users, (b) environmental regulations as the process can waste products and/or generate emissions that may have impact on the environmental, (c) energy efficiency regulations as it may require the reduction of carbon emissions associated with the process, (d) licensing regulations for operators, (e) reporting regulations on process performance and emissions to ensure compliance with established standards, (f) waste management regulations to address the handling, treatment, and disposal of waste materials, and (g) transportation and storage regulations of materials or products for safety and security reasons.

Thermal spray coatings typically contain materials that are subject to regulations related to environmental impact, workplace safety, testing methods, materials specifications, quality control, and other considerations. Standards (such as ISO 14922:2021¹⁰⁷) specifies quality requirements for manufacturers of thermal sprayed coatings to ensure quality assurance for activities in the field of production. While other standards (such as ISO 2063-2:2017¹⁰⁸) specifies requirements for corrosion protection of steel structures (between 50 and 200°C temperature range), which are coated by thermal spraying of zinc, aluminium, or their alloys. It specifies requirements for coating thickness, minimum adhesive strength and surface conditions, surface preparation, thermal spraying, testing, post treatments, and manufacturing locations (workshop, on-site and for repair on-site after assembly). Additionally, there are guidance¹⁰⁹ which provide notes about thermal spraying of metal coatings and metal compound coatings, when 20 or more tonnes are sprayed in any 12 months. There are numerous thermal spray related specifications and standards,¹¹⁰ however, there are no specific regulations on the application of thermal spray coatings for thermochemical cycle molten salt structural parts. It is always possible and essential to ensure compliance with known regulations, consider industrywide practices, work with regulatory agencies, seek guidance where necessary, and maybe there is opportunity to develop specific thermal spray guidance and standards for thermochemical cycle molten salt structural parts application.

4.6 | General innovation and opportunity

Efforts to ramp up hydrogen production and its usage are increasing in many nations, emphasizing larger-scale, more power system-friendly electrolysis. Significant cost reductions must be made to achieve an economically sustainable route for hydrogen production. One of the major factors that can be optimized is the electrolyser efficiency. In addition, the material choice significantly affects the durability of the electrolyser. The electrical efficiency of the electrolyser could achieve values higher with high operating temperatures. The required reduction of costs can only be achieved through continuous material performance improvement.

The major concern with current large installations of novel electrolyser-based hydrogen is that the return-on-investment cost is quite low for the smaller amounts of hydrogen produced. Several factors contribute to this, including the scale and degree of mass-production. Electrolyser system costs start to converge at high operating hours, meaning that the hydrogen economy becomes sustainable as the durability of the electrolyser becomes higher. Thermochemical electrolysis techniques could potentially make a direct impact in addressing this challenge.

Further research is needed pertaining to the optimisation of the material properties to enhance the durability and efficiency of thermochemical cycle electrolysers. The integration of data modeling methods with analytical and numerical methods of process modeling shall enable the creation of full life cycle estimates of the various components of the chosen electrolyser design. Not only is this critically important to ensure the rapid development of electrolyser materials, but it will also have a direct impact on the process and material development costs associated with incremental changes in the electrolyser efficiency. The operational durability of thermochemical cycle electrolyser components is expected to improve to have a self-sustaining and flexible energy production model. This can only be possible through sustained and focused efforts to improve the complete energy production process starting from material development to energy delivery. In a cost analysis report of hydrogen production with different technologies, the Hydrogen Council predicts a cost reduction of 60%–80% due to the advent of large-scale manufacturing of electrodes by 2030.¹¹ The current practice of manual

fabrication is expected to be replaced by automated and streamlined production processes. This requires support from R&D in optimizing the catalyst loading, increased system sizes and associated benefits. Increasing the electrolyser system size to 80–100 MW is projected to reduce the cost from 2 USD/kg of hydrogen produced to 0.5 USD/kg by a conservative estimate. It is also predicted that an increase in the electrolyser efficiency through a reduction in the operating voltage could lead to a cost reduction of 0.4 USD/kg. Also, improved operational and maintenance (O&M) protocols and reduced need for O&M due to better optimized catalyst/electrolyte combinations could lead to a cost reduction of 0.2 USD/kg of hydrogen.

Through further research, the aim could also be to address these critical issues through extensive process modeling and design. To aid the efficiency enhancements of such electrolysers, in this research field, one should consider creating an extensive database of materials, their manufacturing process, characterization methods and observed microstructural features, electrolyser performance and efficiency. This database should be made available to the wider network of energy researchers and key stakeholders in the energy transition process. This will significantly aid in the development of novel materials through the creation of process maps and predicted electrolyser performance using data science. The developed numerical, data analytics and analytical models could also be made available through an open access repository that shall significantly aid researchers in the field of hydrogen production in understanding the effects of design parameter choices on the performance of the electrolyser.

5 | CONCLUDING REMARKS

Since thermochemical cycles operate at high temperatures in a corrosive and harsh environment, the structural (construction) and coating materials require special considerations. Thermally sprayed coatings of specialized feedstock materials (with high thermodynamic resistance) such as superalloys, ceramics, and refractory metals have been considered for such harsh environments as the most suitable materials (on metallic structures) for high temperature corrosive environments. Also, there are multiple lessons learnt related to materials degradation which could be relevant for various thermochemical cycle applications.

Assessment indicated that very limited sets of coating-substrate system with metallic interlayer is likely to survive high temperature corrosive environment for extended period of testing. Penetration of molten salt is possible in coatings which typically contain various types of inherent defects, for example, incompletely filled pores, inter-splat pores and intra-splat microcracks. The failure of coating materials due to high temperature molten salt corrosion were multi-mode in nature (i.e., deformation, fracture, and delamination). These failures were due to the asymmetric material configuration, as well as extension of a small defect which could be accidentally included during material processing, manufacturing, and mechanical, thermal, and chemical stress generation during operation. Over time, these failures modes ultimately degrade the performance of the reactor, leading to the system failure.

Range of techniques could be used to fabricate high temperature corrosion resistant coatings. However, thermal spray coating techniques can help spray feedstock materials where microstructure (e.g., porosity, crystallographic texture, phases, anisotropy, and strains) can be controlled using selection (also called optimized) of spray process parameters. In the published literature, the spray process parameters were developed and optimized (mainly the microstructures, porosity, roughness, and splats size), largely to maximize corrosion resistant properties of the coatings. While fabricating thermally sprayed coatings, it has been a common practice to make changes in spray angle (normal/off normal) to substrate that can also help unique microstructures which leads to varied active surface area. Varied active surface area could help mitigate some of the thermochemical corrosion reaction issues. Overall, it is recommended to develop coatings with low porosity (using spray techniques which offers dense coatings, e.g., HVOF, SPS, and SPPS) and high lamellar cohesion, as the lamellar boundaries act as corrosion paths, and any detachment of the lamellas could lead to coatings degradation in molten salt corrosion conditions. It was proposed to manufacture a metallic inter-layer coating as a means of minimizing thermal expansion and stress effects instigated by overlaid brittle layer on a ductile substrate. Avoiding cracks in coating layers (generally attributed to thermal expansion mismatch between the coatings and substrate, and uneven thermal shock), potentially by managing the residual strains and phase transformation in coatings during manufacturing, could also help reducing layer degradation. The strategy to reduce coating degradation should also include developing top brittle layers which are sacrificial, act as diffusion barrier, reduced scale growth, and resistant to molten salts.

Based on published resources, coating materials considered for the molten salt facing parts includes superalloys like variants of nickel–chrome alloys (e.g., Ni–Cr, Ni–20Cr, Ni–50Cr, Ni–57Cr), Ni–49Cr–2Si, Ni–57Cr–Mo–Si–B,

Ni-21Cr-9Mo-Fe, Ni-21Cr-10W-9Mo-4Cu, NiCr-Cr₃C₂, Cr₃C₂-25(Ni-20Cr), Ni-Cr-B-Si, Ni-Cr-B-Si-Fe), variants of super hard steel (Fe-Cr-W-Nb-Mo), variants of iron-aluminium (e.g., Fe₃Al, Fe-15Al-2Cr), cobalt-chrome (Co-Cr-Mo); ceramic like alumina (Al₂O₃), variants of yttria-stabilized zirconia (YSZ), ceria doped yttria-stabilized zirconia (C-YSZ), scandium doped yttria-stabilized zirconia (Sc-YSZ), lanthanum zirconate (LZ) and pyrochlore-fluorite cerium doped lanthanum zirconate (LZC) with YSZ (LZ-LZC/YSZ), gadolinium zirconate (GZ) with YSZ, and lanthanum phosphate (LaPO₄) with YSZ. Example of metallic inter-layer bond coat feedstock materials considered include variants of nickel-chrome alloys (e.g., Ni-Cr-Al-Y, Ni-25Co-20Cr-8Al-4Ta-0.6Y, Co-32Ni-17Cr-8Al-0.5Y), as a means of minimizing thermal expansion and stress effects.

Application of advanced thermal spray techniques, for example, solution or suspension based thermal spray techniques (SPPS/SPS) have resulted in coatings with micrometer to nanometer microstructures. Varied high energy deposits, for example, high temperature (as in air plasma spraying or APS), leads to fully molten feedstock particles, relatively less temperature (as in high velocity oxy-fuel or HVOF), leads to partially or un-molten feedstock particle, whereas significantly less temperature or near room temperature (as in cold gas dynamic spray or CGDS), leads to minimal oxidation with highly deformed sprayed feedstock particles. Therefore, the coating deposits with flattened feedstock particles (deformed-fully or partially, or combination of both) can be developed leading to different microstructures and roughness depending on process parameters and spray techniques used. The process parameters and spray techniques could also lead to varied through-thickness residual strains (compressive, tensile, or combination of both) in coating-substrate system which in turn could impact overall coating properties.

Lack of solutions utilizing the thermochemical technique for electrolysis does not permit commercial exploitation so far. There is a need to carry fundamental research that could help overcome present challenges and assess opportunities that will unlock efficient hydrogen production with stable thermochemical cycles for operation at Molten Salt Reactor (MSR) nuclear plants. Testing and qualification of materials (coatings, substrates) require specialized equipment and procedures, as such testing is typically carried out for an extended period to study the effect of molten salt. In such work, the coatings are typically exposed to the conditions within an MSR for an extensive period (~100–500 h or more) in the absence of oxygen. It also requires designing a new geometry of sample so that coating integrity on the sharp edge of the sample could be mitigated, and where the immersion tests of samples can be conducted for extended period. Such a test set-up should help evaluate and compare the results of various corrosion resistant coatings after immersion tests and other characterization and monitoring studies.

Some of the know-how, and new design of thermal spray coatings could be useful for thermochemical cycle structural part applications. The example applications included thermal spray coating when tested in aggressive corrosive environment at high temperature, such as nuclear reaction vessels, boiler, waste incinerators, aero engine gas-turbine, and so on. As of now, thermally sprayed coatings present some inherent challenges, for example, deterioration (corrosion, cracking, and reduced residual strength), low mechanical strength, and effect of high operating temperature. Not much research has been carried to investigate the long-term structural stability of the coating-substrate system in thermochemical cycle applications, as well as their life cycle assessment. To develop a technology demonstrator in relation to thermochemical cycle structural parts, among others metallic alloys, perhaps selective materials (i.e., 2¹/₄Cr-1Mo and 9Cr-1Mo steels, stainless steel 304, stainless steel 316, and Incoloy 800H, Hastelloy N) may be adequate, as such materials are currently fully code-qualified for nuclear construction if the operating temperature is restricted. However, the combination of high performing substrate and coating materials (including those possible via additive manufacturing, laser cladding, and powder metallurgy routes) still requires research, potentially leading to fully code-qualified thermochemical cycle constructions (for electrolyser).

There is a need to benchmark thermochemical electrolysis cell materials, design, and operational configurations, if considering for nuclear reactor applications. It also requires developing numerical and computational modeling for reliable design of materials and manufacturing processes, scalable manufacturing, and effective quality control. Issues such as operating conditions in a radiological and chemical environment, restricted access, reduced cost, enhanced structural integrity aligned to regulatory standards, enhanced efficiency, materials selection, and accounting for corrosion rates and degradations needs to be considered. There is a need to have standards or data to support any qualification of structural and coating materials for molten salt reactor thermochemical cycle. If above is not addressed adequately, then it is expected that barriers will be in the adoption, implementation, and sustaining of the new technology. However, this could be overcome through incremental research, and through the provision of awareness, training, and resource allocation.

AUTHOR CONTRIBUTIONS

Nadimul Haque Faisal: Conceptualization; funding acquisition; investigation; methodology; project administration; supervision; validation; writing – original draft; visualization. **Vinooth Rajendran:** Writing – review and editing; data curation. **Anil Prathuru:** Writing – review and editing; funding acquisition. **Mamdud Hossain:** Funding acquisition; writing – review and editing. **Ramkumar Muthukrishnan:** Writing – review and editing. **Yakubu Balogun:** Writing – review and editing. **Ketan Pancholi:** Writing – review and editing. **Tanvir Hussain:** Writing – review and editing. **Siddharth Lokachari:** Writing – review and editing. **Bahman Amini Horri:** Writing – review and editing. **Mark Bankhead:** Writing – review and editing.

ACKNOWLEDGMENTS

Authors (NF, AP, and MH) acknowledges thermochemical electrolysis related funding by UK National Nuclear Laboratory (NNL) via gamechanger Grant No. GC 596 (THERMOSIS), and funding by Henry Royce Institute via Materials Challenge Accelerator Programme Grant No. MCAP034 (METALYSIS). The authors (NF, AP, MH, and BAH) acknowledge high temperature steam electrolysis related funding by the UKRI EPSRC via Grants No. EP/W033178/1 (METASIS). NF also acknowledge ScotGov's Emerging Energy Transition Fund (EETF) via Grant No. EETF/HIS/APP/007 (Hy-One). Also, the author (BAH) acknowledges the funding support provided by the Leverhulme Trust Research Fellowship (LTRF2021\17131) related to redox hydrothermal reactor for production of green hydrogen.

CONFLICT OF INTEREST STATEMENT

The authors declare no conflicts of interest.

PEER REVIEW

The peer review history for this article is available at <https://www.webofscience.com/api/gateway/wos/peer-review/10.1002/eng2.12947>.

DATA AVAILABILITY STATEMENT

Data sharing is not applicable to this article as no new data were created or analyzed in this study.

ORCID

Nadimul Haque Faisal  <https://orcid.org/0000-0001-5033-6336>

REFERENCES

1. Khamis I. Toolkit on Nuclear Hydrogen Production, IAEA, 2019-20. 2020.
2. Kupitz J, Podest M. Nuclear heat applications: world overview. *IAEA Bulletin*. 1984;26(4):18-21. <https://www.iaea.org/sites/default/files/publications/magazines/bulletin/bull26-4/26404781821.pdf>
3. Peakman A, Merk B. The role of nuclear power in meeting current and future industrial process heat demands. *Energies*. 2019;12(19):3664. doi:10.3390/en12193664
4. Roper R, Harkema M, Sabharwall P, et al. Molten salt for advanced energy applications: a review. *Ann Nuclear Energy*. 2022;169:108924. doi:10.1016/j.anucene.2021.108924
5. Waldrop MM. Nuclear technology abandoned decades ago might give us safer, smaller reactors. *Discover Magazine*. February 26, 2019. <https://www.discovermagazine.com/environment/nuclear-technology-abandoned-decades-ago-might-give-us-safer-smaller-reactors>
6. Mallapaty S. China prepares to test thorium-fuelled nuclear reactor. *Nature*. 2021;597(7876):311-312. <https://www.nature.com/articles/d41586-021-02459-w>
7. Calderoni P, Cabet C. Corrosion issues in molten salt reactor (MSR) systems. *Nuclear Corrosion Science and Engineering*. Woodhead Publishing; 2012:842-865. doi:10.1533/9780857095343.6.842
8. El-Emam RS, Ozcan H, Zamfirescu C. Updates on promising thermochemical cycles for clean hydrogen production using nuclear energy. *J Clean Prod*. 2020;262:121424. doi:10.1016/j.jclepro.2020.121424
9. Nuclear Decommissioning Authority (NDA) Factsheet. Operating a nuclear power reactor. 2014 <https://ukinventory.nda.gov.uk/wp-content/uploads/2014/01/Fact-sheet-operating-a-nuclear-power-reactor.pdf>
10. Bryson-Jones H, Bollet Y. New Royce landscape report: Materials for nuclear enabled hydrogen, a landscape report exploring the technologies, recommended research, and wider enablers for the development of a nuclear enabled hydrogen sector. 2023 <https://www.royce.ac.uk/news/new-royce-landscape-report-materials-for-nuclear-enabled-hydrogen/>
11. Hydrogen Council. Path to hydrogen competitiveness: a cost perspective. 2020 https://hydrogencouncil.com/wp-content/uploads/2020/01/Path-to-Hydrogen-Competitiveness_Full-Study-1.pdf

12. Markets and Markets. Hydrogen generation market global forecast to 2028. Accessed February 2024 2024 <https://www.marketsandmarkets.com/Market-Reports/hydrogen-generation-market-494.html>
13. Custom Market Insights. Global water electrolysis market 2023–2032. Accessed February 2024 2024 <https://www.custommarketinsights.com/report/water-electrolysis-market/>
14. Zhiznin SZ, Timokhov VM, Gusev AL. Economic aspects of nuclear and hydrogen energy in the world and Russia. *Int J Hydrogen Energy*. 2020;45(56):31353–31366. doi:10.1016/j.ijhydene.2020.08.260
15. Global Market Insights. Hydrogen generation market to hit \$160 billion by 2026, says global Market Insights, Inc. 2020. Accessed July 2021 <https://www.globenewswire.com/en/news-release/2020/04/01/2009765/0/en/Hydrogen-Generation-Market-to-hit-160-billion-by-2026-Says-Global-Market-Insights-Inc.html>
16. IAEA. Challenges related to the use of liquid metal and molten salt coolants in advanced reactors, IAEA-TECDOC-1696, May. 2013, ISBN: 978-92-0-139910-6. <https://www.iaea.org/publications/8942/challenges-related-to-the-use-of-liquid-metal-and-molten-salt-coolants-in-advanced-reactors>
17. Johnson SC, Davidson FT, Rhodes JD, et al. Selecting favorable energy storage technologies for nuclear power. *Storage and Hybridization of Nuclear Energy*. Academic Press; 2019:119-175. doi:10.1016/B978-0-12-813975-2.00005-3
18. Dolan, T. J., 2017. *Molten Salt Reactors and Thorium Energy*, Woodhead Publishing, ISBN 978-0-08-101126-3. <https://www.sciencedirect.com/book/9780081011263/molten-salt-reactors-and-thorium-energy#book-description>
19. Molten Salt Reactors. IAEA. 2014 <https://www.iaea.org/topics/molten-salt-reactors>
20. Elder R, Allen R. Nuclear heat for hydrogen production: coupling a very high/high temperature reactor to a hydrogen production plant. *Prog Nuclear Energy*. 2009;51(3):500-525. doi:10.1016/j.pnucene.2008.11.001
21. Fujiwara S, Kasai S, Yamauchi H, et al. Hydrogen production by high temperature electrolysis with nuclear reactor. *Progress in Nuclear Energy*. 2008;50(2–6):422-426. doi:10.1016/j.pnucene.2007.11.025
22. Hercog J, Kupecki J, Świątkowski B, et al. Advancing production of hydrogen using nuclear cycles: integration of high temperature gas-cooled reactors with thermochemical water splitting cycles. *Int J Hydrogen Energy*. 2023;52:1070-1083. doi:10.1016/j.ijhydene.2023.06.333
23. Yan XL, Hino R, eds. *Nuclear Hydrogen Production Handbook*. 1st ed. CRC Press; 2011.
24. Steinfeld A. Solar thermochemical production of hydrogen—a review. *Solar Energy*. 2005;78(5):603-615. doi:10.1016/j.solener.2003.12.012
25. Funk JE. Thermochemical hydrogen production: past and present. *Int J Hydrogen Energy*. 2001;26(3):185-190. doi:10.1016/S0360-3199(00)00062-8
26. Carty RH, Mazumder M, Schreider JD, Panborn JB. Thermochemical hydrogen production, Gas Research Institute for the Institute of Gas Technology, GRI Report 80–0023, vol. 1, Chicago, IL 60616. 1981.
27. Knoche KF, Schuster P, Ritterbex T. Thermochemical production of hydrogen by a vanadium/chlorine cycle. Part 2: experimental investigation of the individual reactions. *Int J Hydrogen Energy*. 1984;9(6):473-482. doi:10.1016/0360-3199(84)90099-5
28. Ping Z, Laijun W, Songzhe C, Jingming X. Progress of nuclear hydrogen production through the iodine–sulfur process in China. *Renew Sustain Energy Rev*. 2018;81(2):1802-1812. doi:10.1016/j.rser.2017.05.275
29. Naterer GF, Suppiah S, Stolberg L, et al. Progress of international hydrogen production network for the thermochemical Cu–Cl cycle. *Int J Hydrogen Energy*. 2013;38(2):740-759. doi:10.1016/j.ijhydene.2012.10.023
30. Farsi A, Dincer I, Naterer GF. Review and evaluation of clean hydrogen production by the copper–chlorine thermochemical cycle. *J Clean Prod*. 2020;276:123833. doi:10.1016/j.jclepro.2020.123833
31. Naterer GF, Suppiah S, Rosen MA, et al. Progress in thermochemical water splitting with the Cu–Cl cycle for hydrogen production, Corpus ID: 201031462. 2019 <https://research.library.mun.ca/13441/1/2015-IJHEb.pdf>
32. Naterer GF, Suppiah S, Rosen MA, et al. Advances in unit operations and materials for the CuCl cycle of hydrogen production. *Int J Hydrogen Energy*. 2017;42(24):15708-15723. doi:10.1016/j.ijhydene.2017.03.133
33. Ozcan H, El-Emam RS, Horri BA. Thermochemical looping technologies for clean hydrogen production – current status and recent advances. *J Clean Prod*. 2023;382:135295. doi:10.1016/j.jclepro.2022.135295
34. Eklund J, Phother J, Sadeghi E, Joshi S, Liske J. High-temperature corrosion of HVOF-sprayed Ni-based coatings for boiler applications. *Oxid Metals*. 2019;91(5):729-747. doi:10.1007/s11085-019-09906-0
35. Ghandehariun S. Thermal management of the copper–chlorine cycle for hydrogen production: analytical and experimental investigation of heat recovery from molten salt [online]. PhD Dissertation. University of Ontario Institute of Technology, Canada. 2012 <https://hdl.handle.net/10155/271>
36. Siantar E. Study of the effect of molten CuCl immersion test on alloys with high Ni-content with and without surface coatings [Online]. University of Ontario Institute of Technology, Canada. 2012 <https://hdl.handle.net/10155/232>
37. Sridharan K, Allen TR. Corrosion in molten salts. *Molten Salts Chemistry*. Elsevier; 2013:241-267. doi:10.1016/B978-0-12-398538-5.00012-3
38. Li C, Lei G, Liu J, Liu A, Ren CL, Huang H. A potential candidate structural material for molten salt reactor: ODS nickel-based alloy. *J Mater Sci Technol*. 2022;109:129-139. doi:10.1016/j.jmst.2021.08.071
39. Wright RN, Sham TL. Status of metallic structural materials for molten salt reactors (No. INL/EXT-18-45171-Rev000). Idaho National Lab. (INL), Idaho Falls, ID (United States); Argonne National lab. (ANL), Argonne, IL (United States). 2018. doi:10.2172/1467482
40. David H. Module 5: Materials (Presentation on Molten Salt Reactor Technology, 7–8 November. 2017 <https://www.nrc.gov/docs/ML1733/ML17331B117.pdf>

41. Baykara SZ. Hydrogen production by direct solar thermal decomposition of water, possibilities for improvement of process efficiency. *Int J Hydrogen Energy*. 2004;29(14):1451-1458. doi:10.1016/j.ijhydene.2004.02.014
42. Norbeck J, Durbin T, Heffel J, Montano M. *Hydrogen fuel for surface transportation*. SAE International; 1996.
43. Holladay JD, Hu J, King DL, Wang Y. An overview of hydrogen production technologies. *Catal Today*. 2009;139(4):244-260. doi:10.1016/j.cattod.2008.08.039
44. Xie J, Wang X, Li A, Li F, Zhou Y. Corrosion behaviour of selected Mn+1AXn phases in hot concentrated HCl solution: effect on an element and MX layer. *Corros Sci*. 2012;60:129-135. doi:10.1016/j.corsci.2012.03.047
45. Wu D, Mao F, Wang S, Zhou Z. A low-temperature fabrication route for enhancing mechanical properties and corrosion resistance of porous mullite ceramics through homogeneously mullite sol-coating method. *J Ceram Process Res*. 2013;14:677-681.
46. Sure J, Shankar A, Ramya S, Mudali U. Molten salt corrosion of high-density graphite and partially stabilized zirconia coated high-density graphite in molten LiCl-KCl salt. *Ceram Int*. 2012;38:2803-2812. doi:10.1016/j.ceramint.2011.11.051
47. Kamali AR, Fray DJ. Molten salt corrosion of graphite as a possible way to make carbon nanostructures. *Carbon*. 2013;56:121-131. doi:10.1016/j.carbon.2012.12.076
48. Vignarooban K, Pugazhendhi P, Tucker C, Gervasio D, Kannan A. Corrosion resistance of hastelloys in molten metal-chloride heat-transfer fluids for concentrating solar power applications. *Solar Energy*. 2014;103:62-69. doi:10.1016/j.solener.2014.02.002
49. Sellers RS, Cheng WJ, Anderson MH, Sridharan K, Wang CJ, Allen TR. Materials corrosion in molten LiF-NaF-KF eutectic salt under different reduction-oxidation conditions. *Proc ICAPP*. 2012;12:24-28.
50. O'Brien JE, Stoots CM, Herring JS, et al. *High temperature electrolysis for hydrogen production from nuclear energy—technology summary* (No. INL/EXT-09-16140). Idaho National Lab.(INL), Idaho Falls, ID (United States). 2010. doi:10.2172/978368
51. Roeb M, Neises M, Monnerie N, et al. Materials-related aspects of thermochemical water and carbon dioxide splitting: a review. *Materials*. 2012;5(11):2015-2054. doi:10.3390/ma5112015
52. Yadav D, Banerjee R. A review of solar thermochemical processes. *Renew Sustain Energy Rev*. 2016;54:497-532. doi:10.1016/j.rser.2015.10.026
53. Babu PS, Madhavi Y, Krishna LR, Sivakumar G, Rao DS, Padmanabham G. Thermal spray coatings for erosion–corrosion resistant applications. *Trans Indian Inst Metals*. 2020;73:2141-2159. doi:10.1007/s12666-020-02053-0
54. Singh S, Berndt CC, Singh RK, Singh H, Ang ASM. Applications and developments of thermal spray coatings for the iron and steel industry. *Materials*. 2023;16(2):516. doi:10.3390/ma16020516
55. Faisal NH, Prathuru A, Ahmed R, et al. Application of thermal spray coatings in electrolyzers for hydrogen production: advances, challenges, and opportunities. *ChemNanoMat*. 2022a;8(12):e202200384. doi:10.1002/cnma.202200384
56. Tejero-Martin D, Rezvani Rad M, McDonald A, Hussain T. Beyond traditional coatings: a review on thermal-sprayed functional and smart coatings. *J Thermal Spray Technol*. 2019;28(4):598-644. doi:10.1007/s11666-019-00857-1
57. Faisal NH, Ahmed R, Prathuru AK, Paradowska A, Lee TL. Measuring residual strain and stress in thermal spray coatings using neutron diffractometers. *Exp Mech*. 2022b;62:369-392. doi:10.1007/s11340-021-00803-9
58. Azhar MS. Evaluation of the Effects of Molten CuCl on Corrosion Resistant Coatings [online]. Master's Dissertation. University of Ontario Institute of Technology, Canada. 2016 <https://hdl.handle.net/10155/731>
59. Azarbayjani K, Rizvi G, Foroutan F. Evaluating effects of immersion tests in molten copper chloride salts on corrosion resistant coatings. *Int J Hydrogen Energy*. 2016;41(19):8394-8400. doi:10.1016/j.ijhydene.2015.10.092
60. Sadeghi E, Markocsan N, Joshi S. Advances in corrosion-resistant thermal spray coatings for renewable energy power plants. Part I: effect of composition and microstructure. *J Thermal Spray Technol*. 2019;28(8):1749-1788. doi:10.1007/s11666-019-00938-1
61. Ma J, Duan Y, Chen W, et al. High temperature tribological properties of the D-gun WC-12Co coating in fluoride molten salt. *Wear*. 2023;530–531:205031. doi:10.1016/j.wear.2023.205031
62. Hussain T, Dudziak T, Simms NJ. Fireside corrosion behavior of HVOF and plasma-sprayed coatings in advanced coal/biomass co-fired power plants. *J Thermal Spray Technol*. 2013;22:797-807. doi:10.1007/s11666-013-9887-x
63. Hussain T, Simms NJ, Nicholls JR, Oakey JE. Fireside corrosion degradation of HVOF thermal sprayed FeCrAl coating at 700–800°C. *Surf Coat Technol*. 2015;268:165-172. doi:10.1016/j.surfcoat.2015.01.074
64. Simms NJ, Sumner J, Hussain T, Oakey JE. Fireside issues in advanced power generation systems. *Mater Sci Technol*. 2013;29(7):804-812. doi:10.1179/1743284712Y.0000000133
65. Wang G, Liu H, Chen T, et al. Comparative investigation on thermal corrosion of alloy coatings in simulated waste incinerator environment. *Corros Sci*. 2021a;189:109592. doi:10.1016/j.corsci.2021.109592
66. Wang Q, Liu C, Luo R, Li X, Li D, Macián-Juan R. Thermo-economic analysis and optimization of the very high temperature gas-cooled reactor-based nuclear hydrogen production system using copper–chlorine cycle. *Int J Hydrogen Energy*. 2021b;46(62):31563-31585. doi:10.1016/j.ijhydene.2021.07.060
67. Leng K, Romero AR, Venturi F, Ahmed I, Hussain T. Solution precursor thermal spraying of gadolinium zirconate for thermal barrier coating. *J Eur Ceram Soc*. 2022;42(4):1594-1607. doi:10.1016/j.jeurceramsoc.2021.11.050
68. Shankar AR, Mudali UK, Sole R, Khatak HS, Raj B. Plasma-sprayed yttria-stabilized zirconia coatings on type 316L stainless steel for pyrochemical reprocessing plant. *J Nuclear Mater*. 2008;372(2–3):226-232. doi:10.1016/j.jnucmat.2007.03.175
69. Lee HY, Baik KH. Comparison of corrosion resistance between Al₂O₃ and YSZ coatings against high temperature LiCl-Li₂O molten salt. *Metals Mater Int*. 2009;15(5):783-787. doi:10.1007/s12540-009-0783-8
70. Uusitalo MA, Vuoristo PMJ, Mäntylä TA. High temperature corrosion of coatings and boiler steels below chlorine-containing salt deposits. *Corros Sci*. 2004;46(6):1311-1331. doi:10.1016/j.corsci.2003.09.026

71. Chatha SS, Sidhu HS, Sidhu BS. High temperature hot corrosion behaviour of NiCr and Cr3C2-NiCr coatings on T91 boiler steel in an aggressive environment at 750 C. *Surf Coat Technol.* 2012;206(19-20):3839-3850. doi:10.1016/j.surfcoat.2012.01.060
72. Sidhu TS, Prakash S, Agrawal RD. Evaluation of hot corrosion resistance of HVOF coatings on a Ni-based superalloy in molten salt environment. *Mater Sci Eng A.* 2006;430(1-2):64-78. doi:10.1016/j.msea.2006.05.099
73. Singh S, Goyal K, Goyal R. Performance of Cr₃C₂-25 (Ni-20Cr) and Ni-20Cr coatings on T91 boiler tube steel in simulated boiler environment at 900°C. *Chem Mater Eng.* 2016;4(4):57-64. <https://www.hrpub.org/download/20160930/CME1-15507544.pdf>
74. Paul S, Harvey MDF. Corrosion testing of Ni alloy HVOF coatings in high temperature environments for biomass applications. *J Thermal Spray Technol.* 2013;22(2):316-327. doi:10.1007/s11666-012-9820-8
75. Oksa M, Tuurna S, Varis T. Increased lifetime for biomass and waste to energy power plant boilers with HVOF coatings: high temperature corrosion testing under chlorine-containing molten salt. *J Thermal Spray Technol.* 2013;22(5):783-796. doi:10.1007/s11666-013-9928-5
76. Mishra NK, Rai AK, Mishra SB, Kumar R. Hot corrosion behaviour of detonation gun sprayed Stellite-6 and Stellite-21 coating on boiler steel SAE 431 at 900°C. *Int J Corros.* 2014;2014:1-4. doi:10.1155/2014/146391
77. Porcayo-Calderon J, Sotelo-Mazón O, Casales-Diaz M, Ascencio-Gutierrez JA, Salinas-Bravo VM, Martinez-Gomez L. Electrochemical study of Ni20Cr coatings applied by HVOF process in ZnCl₂-KCl at high temperatures. *J Analyt Methods Chem.* 2014;2014:1-10. doi:10.1155/2014/503618
78. Liu HF, Xiong X, Li XB, Wang YL. Hot corrosion behavior of Sc₂O₃-Y₂O₃-ZrO₂ thermal barrier coatings in presence of Na₂SO₄+ V₂O₅ molten salt. *Corros Sci.* 2014;85:87-93. doi:10.1016/j.corsci.2014.04.001
79. Kamal S, Jayaganthan R, Prakash S. Evaluation of cyclic hot corrosion behaviour of detonation gun sprayed Cr₃C₂-25% NiCr coatings on nickel-and iron-based superalloys. *Surf Coat Technol.* 2009;203(8):1004-1013. doi:10.1016/j.surfcoat.2008.09.031
80. Loghman-Estarki MR, Razavi RS, Jamali H. Effect of molten V₂O₅ salt on the corrosion behavior of micro-and nano-structured thermal sprayed SYSZ and YSZ coatings. *Ceram Int.* 2016;42(11):12825-12837. doi:10.1016/j.ceramint.2016.05.047
81. Jonnalagadda KP, Mahade S, Curry N, et al. Hot corrosion mechanism in multi-layer suspension plasma sprayed Gd₂Zr₂O₇/YSZ thermal barrier coatings in the presence of V₂O₅ + Na₂SO₄. *J Thermal Spray Technol.* 2017;26(1):140-149. doi:10.1007/s11666-016-0486-5
82. Hajizadeh-Oghaz M, Razavi RS, Ghasemi A, Valefi Z. Na₂SO₄ and V₂O₅ molten salts corrosion resistance of plasma-sprayed nanostructured ceria and yttria co-stabilized zirconia thermal barrier coatings. *Ceram Int.* 2016;42(4):5433-5446. doi:10.1016/j.ceramint.2015.12.085
83. Fan W, Bai Y, Liu YF, et al. Corrosion behavior of Sc₂O₃-Y₂O₃ co-stabilized ZrO₂ thermal barrier coatings with CMAS attack. *Ceram Int.* 2019;45(12):15763-15767. doi:10.1016/j.ceramint.2019.05.063
84. Praveen K, Alroy RJ, Rao DS, Sivakumar G. Hot corrosion behavior of hybrid double-layered LZ/LZC+ YSZ thermal barrier coatings made using powder and solution precursor feedstock. *Surf Coat Technol.* 2022;436:128260. doi:10.1016/j.surfcoat.2022.128260
85. Zhang C, Fei J, Guo L, et al. Thermal cycling and hot corrosion behavior of a novel LaPO₄/YSZ double-ceramic-layer thermal barrier coating. *Ceramic Int.* 2018;44(8):8818-8826. doi:10.1016/j.ceramint.2018.02.057
86. Roche J, Gómez PA, Alvarado-Orozco JM, Toro A. Hot corrosion and thermal shock resistance of dense-CYSZ/YSZ bilayer thermal barrier coatings systems applied onto Ni-base superalloy. *J Eur Ceramic Soc.* 2020;40(15):5692-5703. doi:10.1016/j.jeurceramsoc.2020.07.004
87. ASTM G31-21. Standard guide for laboratory immersion corrosion testing of metals. 2021 <https://www.astm.org/g0031-21.html>
88. Naterer GF, Suppiah S, Stolberg L, et al. Canada's program on nuclear hydrogen production and the thermochemical Cu-Cl cycle. *Int J Hydrogen Energy.* 2010;35(20):10905-10926. doi:10.1016/j.ijhydene.2010.07.087
89. Lamarsh JR, Baratta AJ. *Introduction to Nuclear Engineering.* 3d ed. Prentice-Hall; 2001 ISBN: 0-201-82498-1.
90. Zinkle SJ, Busby JT. Structural materials for fission & fusion energy. *Mater Today.* 2009;12(11):12-19. doi:10.1016/S1369-7021(09)70294-9
91. Zinkle SJ, Was GS. Materials challenges in nuclear energy. *Acta Mater.* 2013;61(3):735-758. doi:10.1016/j.actamat.2012.11.004
92. Hosemann P, Frazer D, Fratoni M, Bolind A, Ashby MF. Materials selection for nuclear applications: challenges and opportunities. *Scr Mater.* 2018;143:181-187. doi:10.1016/j.scriptamat.2017.04.027
93. Yang H. Anisotropic effects of radiation-induced hardening in nuclear structural materials: a review. *J Nuclear Mater.* 2022;561:153571. doi:10.1016/j.jnucmat.2022.153571
94. Zinkle SJ, Terrani KA, Snead LL. Motivation for utilizing new high-performance advanced materials in nuclear energy systems. *Curr Opin Solid State Mater Sci.* 2016;20(6):401-410. doi:10.1016/j.cossms.2016.10.004
95. Biserova-Tahchieva A, Biezma-Moraleda MV, Llorca-Isern N, Gonzalez-Lavin J, Linhardt P. Additive manufacturing processes in selected corrosion resistant materials: a state of knowledge review. *Materials.* 2023;16(5):1893. doi:10.3390/ma16051893
96. Raiman SS, Muralidharan G, Mayes RT, Kurley JM III. *Compatibility studies of cladding candidates and advanced low-Cr superalloys in molten NaCl-MgCl₂* (No. ORNL/TM-2019/1132). Oak Ridge National Lab.(ORNL), Oak Ridge, TN (United States). 2019. doi:10.2172/1507851
97. Zhu H, Ouyang M, Hu J, Zhang J, Qiu C. Design and development of TiC-reinforced 410 martensitic stainless-steel coatings fabricated by laser cladding. *Ceram Int.* 2021;47(9):12505-12513. doi:10.1016/j.ceramint.2021.01.108
98. Colombo KWE, Kharton VV. Reliability analysis of a multi-stack solid oxide fuel cell from a systems engineering perspective. *Chem Eng Sci.* 2021;238:116571. doi:10.1016/j.ces.2021.116571
99. Park JH, Ahn BT. Time-zero failure current measurement for early monitoring of defective metal lines at wafer level. *J Electrochem Soc.* 2002;150(1):G6. doi:10.1149/1.1523414
100. Buechele AC, De Jonghe LC, Hitchcock D. Degradation of sodium β"-alumina: effect of microstructure. *J Electrochem Soc.* 1983;130(5):1042-1049. doi:10.1149/1.2119881

101. Bhandari R, Trudewind CA, Petra Zapp P. Life cycle assessment of hydrogen production via electrolysis: a review. *J Clean Prod.* 2014;85:151-163. doi:10.1016/j.jclepro.2013.07.048
102. Sadhukhan J. Net zero electricity systems in global economies by life cycle assessment (LCA) considering ecosystem, health, monetization, and soil CO₂ sequestration impacts. *Renew Energy.* 2022;184:960-974. doi:10.1016/j.renene.2021.12.024
103. Zhao G, Kraglund MR, Frandsen HL, et al. Life cycle assessment of H₂O electrolysis technologies. *Int J Hydrogen Energy.* 2020;45:23765-23781. doi:10.1016/j.ijhydene.2020.05.282
104. Sadhukhan J, Christensen M. An in-depth life cycle assessment (LCA) of lithium-ion battery for climate impact mitigation strategies. *Energies.* 2021;14(17):5555. doi:10.3390/en14175555
105. Mordor Intelligence. Thermal spray coatings market size and share analysis report, 2024–2029. 2024. Accessed February 2024 <https://www.mordorintelligence.com/industry-reports/thermal-spray-market>
106. Bhattacharyya R, Singh KK, Bhanja K, Grover RB. Assessing techno-economic uncertainties in nuclear power-to-X processes: the case of nuclear hydrogen production via water electrolysis. *Int J Hydrogen Energy.* 2023;48(38):14149-14169. doi:10.1016/j.ijhydene.2022.11.315
107. ISO 14922:2021. Thermal spraying—quality requirements for manufacturers of thermal sprayed coatings. 2021 Accessed December 2023 <https://www.iso.org/obp/ui/en/#iso:std:iso:14922:ed-1:v1:en>
108. ISO 2063-2:2017. Thermal spraying zinc, aluminium and their alloys. Part 2: execution of corrosion protection systems, pp. 1–37. 2017. Accessed December 2023 <https://www.iso.org/standard/61894.html>
109. Process Guidance Note 6/35(13). Statutory guidance for metal powder and other thermal spraying processes. 2013. Accessed December 2023 https://assets.publishing.service.gov.uk/media/5a816b15ed915d74e33fe19d/metal-powder-and-other-thermal-spraying-processes-process-guidance-note-6-35-13_.pdf
110. ASM Thermal Spray Society Specifications and Standards. n.d. Accessed December 2023. <https://www.asminternational.org/tss/technical/specifications/>

How to cite this article: Faisal NH, Rajendran V, Prathuru A, et al. Thermal spray coatings for molten salt facing structural parts and enabling opportunities for thermochemical cycle electrolysis. *Engineering Reports.* 2024;6(9):e12947. doi: 10.1002/eng2.12947